Recent Warming and Watershed Impacts of the Tonle Sap Lake, Cambodia

Kensey Daly

A thesis

submitted in partial fulfillment of the

requirements for the degree of

Master of Science in Civil Engineering

University of Washington

2019

Reading Committee:

Faisal Hossain

Gordon Holtgrieve

Program Authorized to Offer Degree:

Civil and Environmental Engineering

University of Washington

Abstract

Recent Warming and Watershed Imapcts of the Tonle Sap Lake, Cambodia

Kensey Daly

Chair of the Supervisory Committee:
Professor Faisal Hossain
Civil and Environmental Engineering

Tonle Sap Lake in Cambodia is arguably the world's most productive freshwater ecosystems and the dominant source of animal protein for the country. The rapid rise of hydropower schemes, deforestation, land development and climate change impacts in the Mekong River Basin are now reasons of concern for Tonle Sap Lake's ecological health and its role in future food security. We identify significant recent warming of lake temperature and survey how each of these anthropogenic perturbations in Tonle Sap's floodplain and the Mekong River Basin may be influencing this trend. Between 1981 and 2014 the lake's dry-season monthly average temperature increased by 0.03°C $year^{-1}$, largely in-sync with warming trends of the local air temperature and upstream rivers. Impacts of deforestation and agriculture development in the lake's floodplain showed a high correlation with an increase in the number of warm days observed in the lake, particularly in its southeast region (agriculture $R^2 = 0.61$ and deforestation $R^2 = 0.39$). Between

2003 and 2018, 79 dams totaling in 72 km^3 of volumetric capacity were constructed in the Mekong River Basin. This dam development coincided with a decreasing trend in number of dry-season warm days per year in the lower Mekong River, while Tonle Sap Lake's number of dry-season warm days continued to increase. This study revealed that Tonle Sap Lake's temperature trends are highly influenced by temperature trends in local climate, agriculture development and deforestation of the lake's watershed. Although there was no noticeable impact observed of upstream dam development in the Mekong basin, local-to-regional agricultural and land management of the lake's watershed appear as effective strategies for maintaining a stable thermal regime in the lake for maximum ecosystem health.

TABLE OF CONTENTS

LIST OF FIGURES

LIST OF TABLES

ACKNOWLEDGEMENTS

This work was supported by National Science Foundation project NSF EAR 1740042 titled INFEWS/T1: Linking Current and Future Hydrologic Change to Hydropower, Human Nutrition, and Livelihoods in the Lower Mekong Basin. The authors thank Ben Miller and Asian Disaster Preparedness Center for providing in-situ temperature data.

Chapter 1. INTRODUCTION

1.1 MOTIVATION

The rapid rise of hydropower development, deforestation, land development and climate change impacts in the Mekong River Basin are reasons of concern for downstream ecosystems such as Tonle Sap Lake, one of the world's most productive freshwater fisheries (Baran & Myschowoda, 2009). Each of these factors are changing and interacting in Tonle Sap Lake's watershed, degrading the water quality where at least 150 fish species, over 200 plant species and 4.2 million human residents are dependent on the lake's resources (Campbell, Poole, Giesen, & Valbo-Jorgensen, 2006; Commission, State of the Basin Report, 2003). Anthropogenic perturbations such as these have been found to disrupt surface water thermal regimes, which can lead to disruption of phenological, geographical and species size distribution (Ilha, Schiesari, Yanagawa, Jankowski, & Navas, 2018). Tropical vertebrate species, including fish, are believed to be particularly at risk of climate warming because they are already at the upper end of known thermal maxima, have evolved with narrower thermal windows, and have limited adaptive capacity (Ilha, Schiesari, Yanagawa, Jankowski, & Navas, 2018; Stillman, 2003; Ficke, Myrick, & Hansen, 2007). Tonle Sap Lake has been a valuable resource to the region since the construction of Angkor Wat near 800 A.D. (Campbell, Poole, Giesen, & Valbo-Jorgensen, 2006) and sustainable management of the lake is vital for local livelihood in Cambodia, shown in Figure 1. Understanding the lake's temperature characteristics can help inform water resource managers to plan and operate infrastructure and natural resources throughout the region so that ecosystem function and human benefits are maintained.

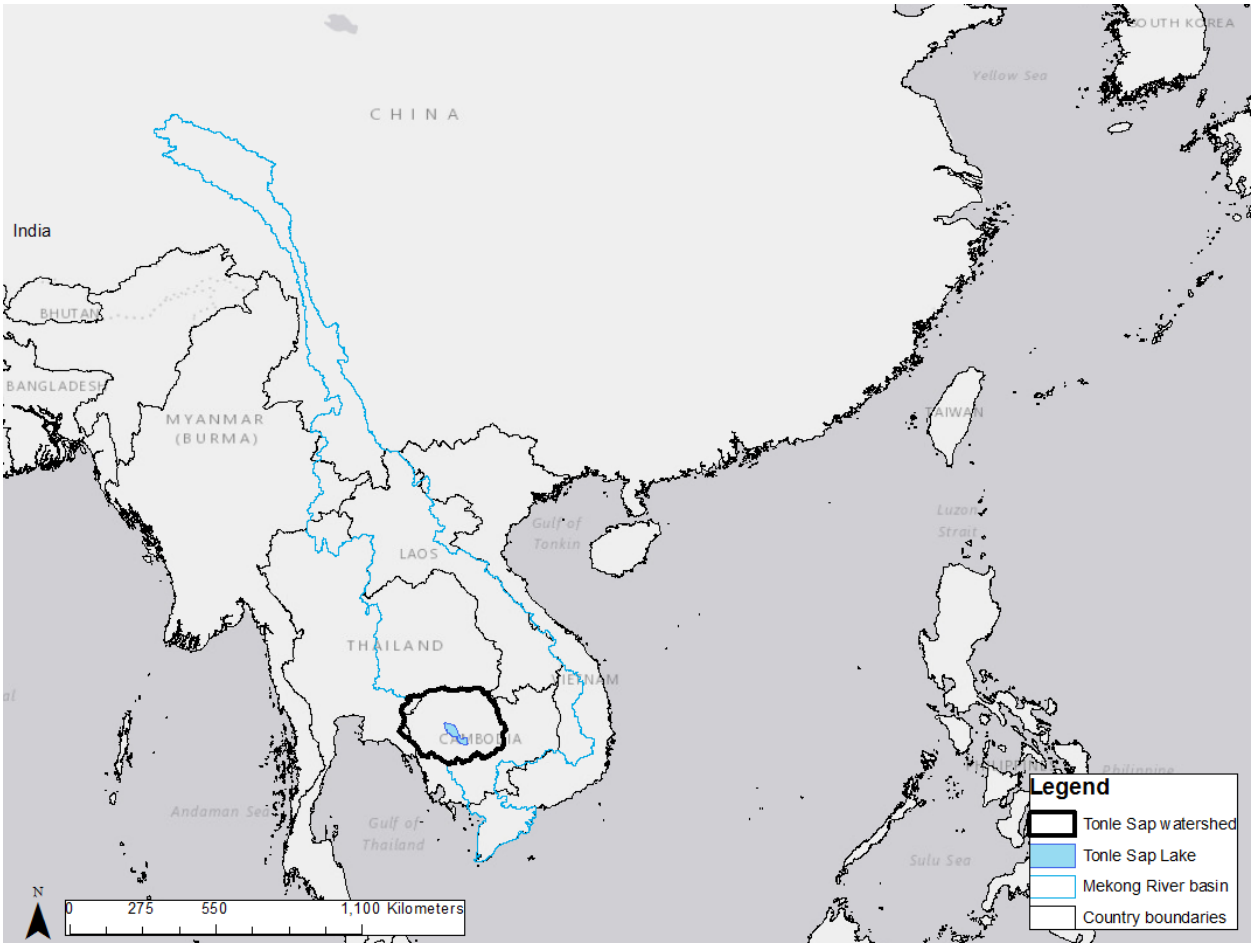

Figure 1.1. Location of Tonle Sap Lake, it's watershed and the Mekong River Basin.

Water temperature regulates many processes in lakes, including both chemical and biological processes. Knowledge of surface water temperature has economic and ecological value because of the important role it serves when considering issues regarding water quality and biotic environments. It is frequently measured as a parameter in stream and lake monitoring efforts to determine the overall health of aquatic ecosystems as thermal pollution is often linked to anthropogenic perturbations (Caissie, 2006). Watershed changes including land cover, climate, and dam development have all shown significant impacts on surface water thermal regimes around the world (Adrian et al., 2009). Deforestation and agriculture can cause warmer surface runoff, thermally polluting downstream water bodies (Brown & Krygier, 1970; Beschta, 1997; Johnson

& Jones, 2000). Dams have been shown to warm or cool downstream waters, depending on the depth from which water is released (Niemeyer, Cheng, Mao, Yearsley, & Nijssen, 2018). Global warming is causing lake temperature around the world to increase (Schneider & Hook, 2010). Therefore, it is critical to understand how changes upstream and throughout the watershed landscape are impacting Tonle Sap's thermal water quality as well. Tonle Sap Lake, its watershed and the Mekong River Basin where a majority of the lake's water flows in from, have undergone rapid changes due to climate change and human activities such as deforestation, agriculture development and dam development (IPCC, 2007; Benger, 2009; MRC and UNEP, 1997). Close to 50 million residents living upstream influence the lake's water quality, through economic activities such as agriculture, logging, urbanization and industrialization that are rapidly degrading the watershed (Yen et al., 2007).

There is a broad concern over the recent decline in fish population and size in Tonle Sap Lake (van Zaline, 2002; Hortle, 2007). Fish provide most of animal protein and vitamin A (>80%) to Cambodians (Hortle, 2007). The exact cause of the observed change to the fishery is unknown, but it is imperative that ecological conditions which provide stable ecosystem services to the region persist. Dam development has already had a greater impact on Tonle Sap's hydrological regime than any other human impact (Cochrane, Arias, & Piman, 2014). Dams are expected to decrease the average maximum wet season water level and increase the dry season water level over time, and some of these hydrologic impacts have already been observed (Cochrane, Arias, & Piman, 2014; Kummu & Sarkkula, 2008). A modest rise in the dry season lake water level would permanently immerse disproportionally large areas of the floodplain, resulting in permanent flooding of valuable land that supports farming operations and ecologically important gallery forests (Kummu & Sarkkula, 2008). Land cover changes such as deforestation and irrigation

schemes also impact the lake's natural systems. Around Tonle Sap Lake, most forested areas have been cleared for farming, settlements and timber harvesting, altering the land cover around the permanent lake boundaries (Campbell, Poole, Giesen, & Valbo-Jorgensen, 2006). Development of large-scale irrigation schemes are anticipated to grow and divert significant flow from the Mekong River (Kummu et al., 2014).

While impacts to Tonle Sap's hydrological regime from dam development in the Mekong Basin have been observed, impacts to its thermal regime are still unknown. Inundating larger portions of the floodplain inevitably alters the energy and thermal balance of the region. Both deforestation and shifts in agriculture operations alter surface energy and local water budgets, directly impacting nearby surface water systems (Sahin and Hall, 1996; Adrian et al., 2009). A modelling study in the Mekong River Basin indicates that increased irrigation results in decreased streamflow, increased evapotranspiration and locally significant lower surface temperatures by 0.04 °C on average annually (Haddeland, Lettenmaier, & Skaugen, 2006). Observed impacts through historical data analyses of dam development, climate change and land cover changes are still largely unknown on Tonle Sap Lake.

Climate change impacts in Tonle Sap are also expected to become more significant in the long term (Cochrane, Arias, & Piman, 2014). Manton et al. (2001) studied extreme daily temperature and rainfall trends from 1961 – 1998 and found significant increasing trends in the annual number of hot days and nights and decreasing trends in the annual number of cool days and nights throughout Southeast Asia. Sea level rise is another impact of climate change that is expected to increase the Mekong River delta water level, as well as the river level all the way up to Tonle Sap Lake (Wassmann, Hien, & Hoanh, 2004). This warming trend is not unique to Southeast Asia, and as lake temperature is closely linked to atmospheric conditions, lakes around

the world are warming (Schneider and Hook, 2010). How such changes will translate to the lake and the implications for the fishery are, however, unknown. Furthermore, direct observations of physical and biological conditions over time are extremely limited for the Tonle Sap and the Mekong, in part because of the regions' troubled social and political history. Resilient and adaptive water and natural resource management at Tonle Sap Lake therefore requires new observation methods for understanding recent ecological change so as to better manage the Tonle Sap Lake's future.

The historical abundance of these resources will continue to be at risk of deterioration as population growth and socioeconomic development continues to rise. Various studies have begun deciphering the impacts of anthropogenic activities on Tonle Sap Lake's hydrological characteristics, but there is still much to be understood on impacts to the lake's water quality (Bonheur and Lane, 2002; Cochrane et al., 2016). Surface water temperature provides insight on how changes in Tonle Sap's watershed are impacting the lake's water quality, as a lake's epilimnetic temperature is directly influenced by a watershed's characteristics. Air temperature and climate forcings are highly linked to a lake's epilimnetic temperature, however, other changes in a lake's watershed may confound impacts directly related to climate change. Changes in forest, agricultural and hydrological patterns from human activity also influence the epilimnetic temperature (Adrian et al., 2009). Thus, a change in thermal trends can shed light on how the various human activities are impacting the lake's overall water quality. Understanding of impacts on Tonle Sap's water quality from each of these anthropogenic perturbations is fundamental for long-term resource management planning in Tonle Sap Lake.

While many studies have examined how these changes have impacted the lake's flood regime and biota systems, the purpose of this study is to determine what impacts are driving Tonle

Sap Lake's water quality degradation. From the standpoint of water resource management, fundamental understanding of impacts to the lake's thermal regime can provide insight to drivers of change in the lake's water quality and help prioritize areas where management practices may need to be monitored or improved. Temperature can be used as an indicator and also an integrator of the magnitude and direction that upstream changes may be having on a lake. Lake water surface temperature (LWST) data from space is leveraged for this study, as it has been analyzed for over a hundred lakes around the world (Schneider and Hook, 2010). It is an indicator of anthropogenic and natural perturbations as it is highly sensitive to changes in the surrounding catchment (Williamson et al., 2009; Adrian et al., 2009). Temperature trends are evaluated to understand the potential connection of these trends to human activities and regional trends in climate.

The relentlessly changing forms of civilization in Tonle Sap's watershed has also pressured the lake to become well acquainted with the concept of change, beyond what naturally occurs. Before the lake became connected to the Mekong River 7.5 – 5.5 thousand years ago, it was a much smaller lake (Campbell, Poole, Giesen, & Valbo-Jorgensen, 2006). When it finally connected to the Mekong and grew into the "Great Lake" that it is today, it was a central resource to the construction of Angkor Wat near 800 A.D. (Campbell, Poole, Giesen, & Valbo-Jorgensen, 2006). Tonle Sap's thriving community has prevailed for centuries as kingdoms rose and fell along its shores, European countries extended control over its land, endless hostilities and battles took place on and near its water, brutal communist regimes and decades of international war tore apart its resources. The ability to protect the lake has come a long way since those tumultuous times, but improvement in natural resource management still has a way to go.

1.2 STUDY OBJECTIVES

This study uses space-based remote sensing techniques to estimate previously unavailable long-term water surface temperature trends in the Tonle Sap Lake that have occurred as a result of natural and anthropogenic changes in its surrounding watershed. Water temperature is a key parameter of many physical processes that sustain the natural resources which are so vital for the regional economy. The objective of this study was to improve understanding of recent temperature trends, the drivers of these trends and how anthropogenic perturbations in the local watershed are impacting temperature. As dam, land and agriculture development continues in the region, changes to local food security are inevitable as alterations to these natural cycles compound in the near and long-term. Identifying trends and understanding the potential drivers of those trends in lake temperature are key to developing appropriate management strategies that are optimized for thermal stability of the Tonle Sap Lake.

Tonle Sap Lake is hydraulically intertwined between one of the largest river basins in the world and one of the most productive coastal fishery systems in the world. Tonle Sap's hydraulic connection to the region through the Tonle Sap and Mekong River confluence makes it a great living laboratory for understanding what impacts to natural resources are occurring throughout the region. Dam and land development, as well as climate change are all occurring upstream of Tonle Sap Lake and their impacts are interplaying in Tonle Sap's waters and ecosystems. Dam development has already impacted Tonle Sap's flood regime, a characteristic particularly important for fish and much of the local ecology and livelihood (Arias et al., 2014; Yen et al., 2008).

1.3 THESIS OUTLINE

The thesis has been organized as follows. Chapter 2 provides a literature review of work conducted in the past on Tonle Sap Lake and it's watershed, how thermal regime processes function and their major drivers in lakes, climate change studies that have occurred in Southeast Asia, land cover and land use, dams, and the application of satellite remote sensing data for estimating lake surface water temperature. Each subsection in Chapter 2 provides context of why this study region was selected, the status of climate change, land cover and dam development in the region and how they impact surface water, and the status of applying satellite remote sensing thermal imagery for estimating lake water surface temperature. Chapter 3 describes the methodology applied in this study in detail. The first section of the chapter describes the sites selected for temperature trend analyses. The ensuing sections describe the data sources and analysis methodologies for characterizing lake water surface temperature, climate (or air temperature), land cover and dam development. Chapter 4 discusses the results of the analyses described in Chapter 3, and Chapter 4 ties the analyses together to infer how anthropogenic perturbations in the watershed are impacting Tonle Sap Lake's thermal regime. Chapter 5 also includes recommendations for further study related to the state of Tonle Sap Lake's thermal regime.

Chapter 2. BACKGROUND WORK

2.1 STUDY REGION

Tonle Sap Lake is centrally located in Cambodia, between the Mekong River and its delta that drains into the South China Sea. Its watershed covers approximately 11% of the Mekong River basin's total area and lies primarily in Cambodia, with 5% located in Thailand (Kummu *et al.*, 2014). The lake's tropical climate and flow regime are typically categorized into two seasons, dry (low-water-level period) and monsoon (high-water-level period). The dry period occurs from November through April, while the monsoon season is between May and October. Temperature variability is relatively small between each season. The lake region's mean monthly maximum and minimum air temperature ranges from approximately 30 – 35 °Celsius (°C) and 20 – 27 °C, respectively. Mean monthly rainfall, however, varies much more between each season ranging from 0 and nearly 300 millimeters. The lake's water temperature ranges from approximately 28 – 32 °C throughout the year on average (Campbell, Poole, Giesen, & Valbo-Jorgensen, 2006).

Most of the lake's water originates from the Mekong River, linked via the Tonle Sap River and its floodplain. Figure 2.3 shows a map of Tonle Sap Lake's connection to the Mekong River through the Tonle Sap River, its 11 other tributaries, its permanent inundation area, its floodplain and a high-level diagram of its water balance. The lake acts as a natural flood control storage system for the Mekong River and drains into the Mekong River Delta and the South China Sea. The water level is primarily controlled by the level in the Mekong mainstem, as it can receive up to 20% of the Mekong's flow in July and August. Kummu et. al (2014) found that approximately 53.5% of annual inflows originate from the Mekong River, 34% from 11 smaller tributaries and 12.5% falls directly in from precipitation. Various studies show that approximately 10-25% of the Mekong's flow originates in China as snowmelt and rainfall, while the lower basin contributes

approximately 75% through rainfall runoff (Ruiz-Barradas & Nigam, 2018). Between the years 1997 and 2004, the average annual inflow to Tonle Sap Lake was 83.1 km^3, ranging between 51.1 km^3 in 1998 (drought year) and 109 km^3 in 2000 (wet year). Approximately 88% of this inflow returns to the Mekong River's delta, accounting for 20-50% of the downstream flow into the delta during the dry season (Kummu and Sarkkula, 2008 and Kummu et al., 2014). The mean annual outflow from the lake to the delta's tributaries is approximately 81.9 km^3, varying from 46 km^3 in 1998 to 111 km^3 in 2000. The other eleven tributaries contribute a varying amount of flow between each of them, depending on the season (Kummu, Jozsa, Sarkkula, & Koponen, 2014).

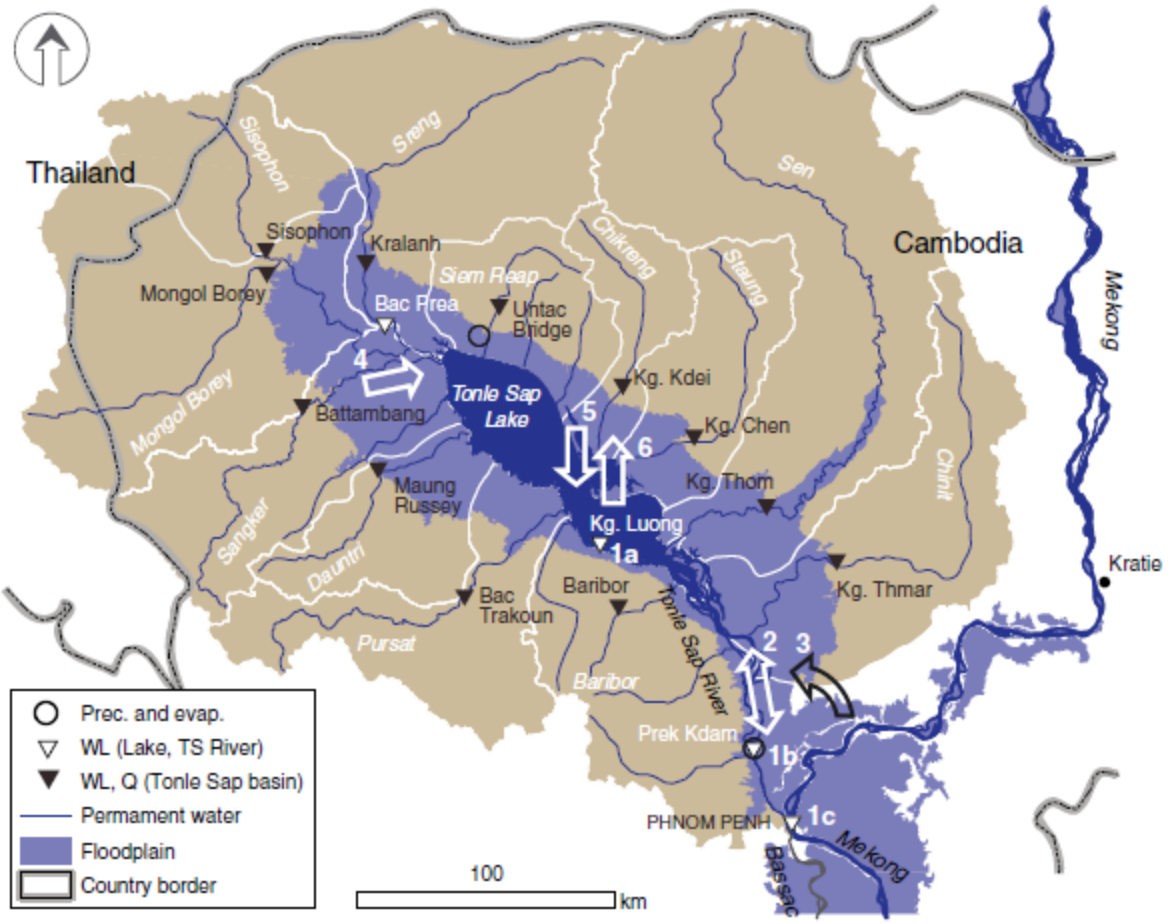

Figure 2.1. Tonle Sap Basin and its sub-catchments with the main rivers (white lines are catchment borders and blue ones are rivers), and floodplain, including the locations of the water balance calculation elements, and hydrological and precipitation measurement sites. Water balance calculation elements: 1a–1c: Water level measurements; 2: Tonle Sap River discharge at Prek Kdam; 3: Overland flow; 4: Flow from tributaries; 5: Precipitation to open water; and 6: Evaporation from open water. Source: (Kummu, Jozsa, Sarkkula, & Koponen, 2014) with permission from John Wiley & Sons, Inc.

The lake's area changes from 2,500 km^2 in the dry season to more than 15,000 km^2 during the peak inflow during the monsoon season, while the depth typically fluctuates between 1.5 and 10 m between the two seasons (Oyagi, Endoh, Ishikawa, Okumura, & Tsukawaki, 2017; Arias, et

al., 2012). The lake's "permanent area" is near 2,400 km^2 with a water level of about 1.44 meters. The average maximum size is near 13,200 km^2 with a depth of about 9.09 meters (Kummu and Sarkkula, 2008). Water level data only exists at Kampong Luong for 1997 – 2009, as well as 1923 – 1965 due to unstable periods of history in Cambodia leading to gaps in available data. The Tonle Sap River flows into the southeast portion, filling the lake up with water directly from the Mekong River during the monsoon season while reversing the flow to carry out Tonle Sap Lake water back to the Mekong River during the dry season (Figure 2.3). The lake is considered to be in the flood-period when the water level is higher than 2.44 meters above mean sea level, only 1 meter higher than the average minimum of 1.33 meters. The timing of the flood peak has historically been consistent; however, the start and end dates of the flood period vary significantly. On average, the flood starts near the end of June, peaks in early October, and ends in the beginning of March. Kummu and Sarkkula (2008) found that during the study period of 1997 – 2005, the flood period ranged from 205 (1998) to 299 (2000) days, the start of the flood varied from 27 May (2000) to 15 June (1998), and the end date varied from 04 February (1998) to 10 April (2004). These findings are shown graphically in Figure 2.4. Monthly average water level and area are shown in Figure 2.5 for the period of 1997 - 2005. The record covers hydrologically extreme events, with a drought occurrence in 1998 and a flood episode in 2000.

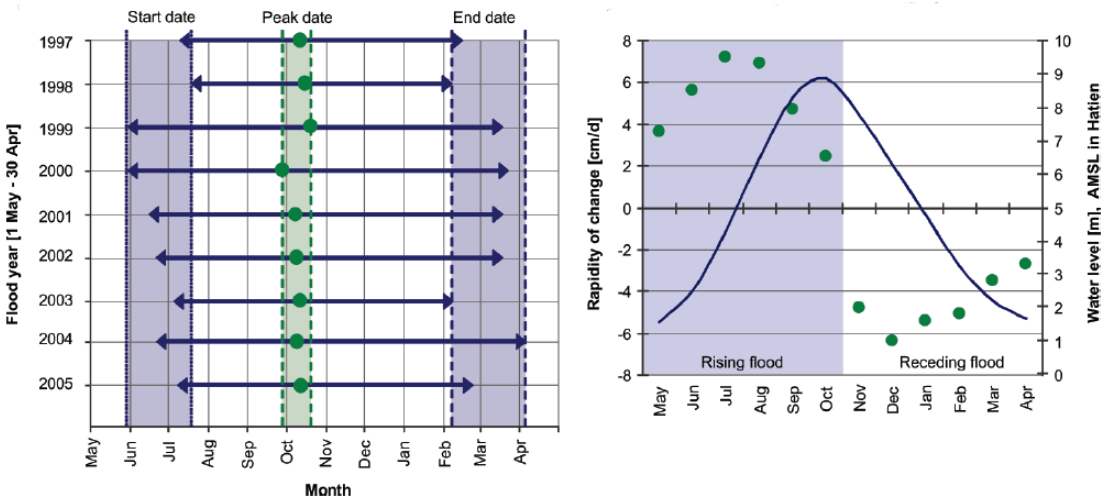

Figure 2.2. (Left) Summary of flood timing, start, end and flood peak date in the Tonle Sap Lake. (Right) Rate of water-level change (green spheres, left vertical axis) and mean monthly water level (continuous line, right vertical axis). The observed minimum and maximum monthly average water levels are illustrated with dotted bars. Source: (Kummu and Sarkkula, 2008) with permission from John Wiley & Sons, Inc.

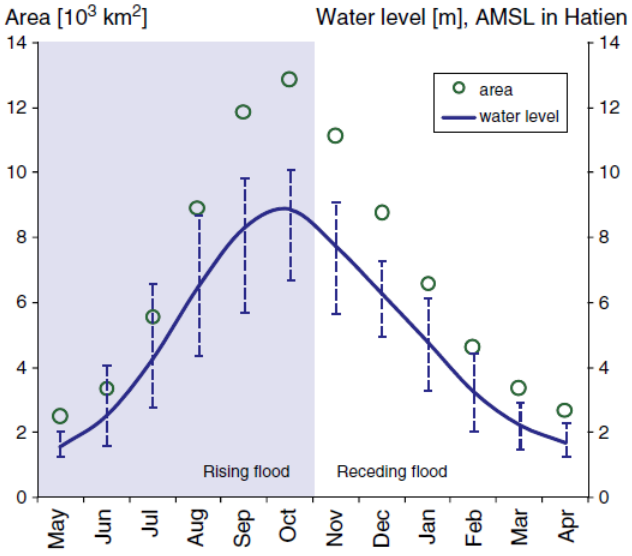

Figure 2.3. Monthly average water level of Tonle Sap Lake at Kampong Luong (continuous line – right vertical axis) and inundated area (circles – left vertical axis). The observed minimum and maximum monthly average water levels have been illustrated with dotted bars. Source: (Kummu et. al., 2014) with permission from John Wiley & Sons, Inc.

The lake's water quality is also characterized uniquely by these two seasons, with a larger water quality influence by the local watershed during low-water-level periods and insignificant anthropogenic impacts observed during monsoon season (Oyagi, Endoh, Ishikawa, Okumura, & Tsukawaki, 2017). Nearly 181,035 km^2 of Tonle Sap's catchment and 4,000 kilometers of the Mekong River flow into Tonle Sap, greatly influencing the water quality of the lake. Close to 50 million residents living upstream influence the lake's water quality, as economic activities such as agriculture, timber logging, urbanization and industrialization are rapidly degrading the watershed. Internal loading has also been found to contribute a significant portion of nutrients to the lake's water column, particularly degrading vegetation in the flood plain. As a result, algal blooms have been observed, as well as other invasive species such as water hyacinth and Mimosa pigra (Yen *et al.*, 2007). However, mixing appears to play a small role on the lake's water quality characteristics because wind velocities are normally relatively low and strong wind events only last a couple of hours. Seiche oscillation is evidently non-existent due to the high friction of the floodplain vegetation (Kummu and Sarkkula, 2008).

From the period of 1995 – 2002, the Mekong River Commission (MRC) launched a water quality monitoring campaign for seven parameters including dissolved oxygen (DO), nitrite + ammonium (NO_3+NH_4), total organic phosphorus (TOP), total suspended sediments (TSS), temperature, pH and conductivity at Kampong Luong monitoring station (location shown in Figure 2.6 as KL). These constituents were also measured monthly at Phnom Peng, Pekdam and Kampong Chhnang (locations shown as white boxes in Figure 2.6). The Water Utilization Program (WUP-FIN) project also launched a monitoring campaign in 2001 and 2002 at 7 sites around the lake. Yen *et al.* (2007) applied an interesting technique to develop annual water quality indices for the period of 1995 – 2002. This technique essentially involved identifying concentration thresholds

and correlations to fish catch data to develop an annual water quality index (WQI) scoring rubric from 1 (poor) to 5 (very good). They also conducted an interesting analysis to compare the water quality data amongst the four MRC stations, and seven WUP-FIN stations.

These analyses revealed several interesting facts about the lake's water quality characteristics and how they compare to those of the Tonle Sap River. First, TSS and conductivity at Kampong Luong generally has a much higher concentration than observed at Kampong Chhnang, Prekdam and Phnom Penh. DO, NO_3+NH_4, and TOP were consistently similar amongst the four stations. At all four MRC stations, DO, pH and conductivity were linearly correlated to each other, as well as TSS and conductivity. TSS was also correlated with pH, DO and temperature at 3 of the MRC's stations, but not at Kampong Luong. However, TSS was positively correlated with NO_3+NH_4 at Kampong Luong. NO_3+NH_4, TOP, temperature and conductivity were strongly correlated between the four stations, but pH, DO and TSS were not strongly correlated between KL and the other three stations. The KL station had the best water quality overall of the 4 stations, potentially because of the surrounding forests and vegetation that help absorb some of the nutrient load. Although many studies indicate 80% of the sediment inflow from the Mekong remained in Tonle Sap, there was not a strong correlation between the KL and PekDam and Phnom Penh stations for TSS.

Comparing the KL station to the seven WUP-FIN stations across the lake and along its shoreline, Yen *et al.* (2007) found that the KL station correlated well with the other stations and was a fair representative for the entire lake, for the purposes of their analyses. It is likely a good representative station because it is located near the middle of the lake in a transition zone between where the Mekong River and northern tributaries waters meet. Any station northwest of KL would be biased towards the quality characteristics of the 11 tributaries, and southeast of this transition

zone would more influenced by the inflow from the Tonle Sap River. Thus, KL station's data was utilized to develop the annual WQI and correlate individual parameters as well as the annual WQI fish catch data. Fish species were categorized into four main biological groups based on nine attributes, including maximum length, growth coefficient, natural mortality, life span, age at first maturity, resilience, main food, trophic level and food consumption. They found that ultimately, all parameter concentrations were negatively correlated to fish catch data. NO_3+NH_4 and pH were not strongly correlated to total dai fish catch, however, their average monthly variations were. DO was only weakly correlated to fish catch, so only TSS, temperature, conductivity, the ratio of N to P, the monthly variation of NO_3+NH_4 and pH were selected for their final analysis. They found that 1996 had the highest WQI of 4.3, while 1998 and 2002 had the lowest WQI of 1 and 1.3, respectively. They also found that generally, smaller, fast-producing fish that have low energy demands had higher catch rates in good WQI rated years than larger, slower-producing fish species with high energy demands. Temperature, pH and NO_3+NH_4 had especially strong correlations to fish catch data. There was a particularly strong positive correlation with the WQI and the *Ciprinidate* fish family, and a particularly strong negative correlation with the *Gyrinocheilidate* family, indicating they are especially sensitive to the Tonle Sap's water quality. The *Gyrinocheilidate* and *Cyprinidate* are especially helpful bioindicators, as they are particularly correlated to the WQI.

Tonle Sap's greatest contribution to its region is its densely vegetated floodplain habitat that provides hatching and nursing grounds for migrant and non-migrant fish species (Sarkkula *et. al*, 2003). The lake's fish stock contributes approximately 60% of Cambodia's total inland catch and 60% of Cambodia's entire protein intake contributing ~$2 billion to the country's economy. At least 178 species have been identified from fish catches during the period of 1995 – 2002 (Yen

et al., 2007). Fish are caught primarily through "dai" fisheries, a method operating along the Tonle Sap River during receding flow conditions. Many of the fish feast on food in the floodplains during the wet season, and many white fish species run back towards the Mekong around 6 days before the full moon where dai fisherman await them (Campbell *et al.*, 2006). Approximately 63-64 dai operated between 1995 – 2012 at 14 locations (Sabo *et al.,* 2017, Yen *et. al.,* 2007). The number of dai is regulated by the Cambodian Department of Fisheries.

The Giant Snakehead fish contributes most of the lake catch, while the dai fisheries are dominated by the small migratory cyprinids (Campbell, Poole, Giesen, & Valbo-Jorgensen, 2006). A majority of fish species belong to four families: Cyprinidae (39%), Bagridae (8%), Siluridae (7%) and Pangasiidae (7%). Prahok is one of the staple fish caught for food for the region, and locals believe their population is declining (Osborne, 2000). Fish stock could appear to be declining to individual fishermen because the fishermen population is also growing, so even if fish stock were stable, there is less fish caught per fisherman over time. Also, the average size of fish caught appears to be decreasing which is a sign of overfishing. It has been claimed that fish diversity is declining, based on fish catch data from 1936-76 and 1995-97, however, there are many weaknesses in this analysis. In addition to fish and vegetation, it is worth mentioning that Tonle Sap is home to 11 globally threatened and 6 near-threatened species of vertebrates, the Siamese Crocodile which has been hunted close to extinction and provides the world's largest harvest of freshwater snakes. Dolphins that were historically observed in the lake can no longer be found due to overfishing since the 1940's (Campbell, Poole, Giesen, & Valbo-Jorgensen, 2006).

Ishikawa *et al.* (2017) developed a model for fishery management in developing countries, utilizing Tonle Sap as a case study because of the community-based management approach. A community-based approach to fishery management provides a stationary fishing gear operation

with licenses from the government, data collection efforts that help scientists reveal the distribution of fish stock and management targets and provides the government with better understanding on fish stock status to set appropriate regulation for fisheries activities. Their study strongly emphasizes the point that a combined local community, scientist and government cooperative effort has proven to be necessary for sustainable fishery and natural resource management.

The vegetation in the floodplain is one of the most important components of the lake's ecosystem and is largely dependent upon the flood pulse patterns that occur in the lake. Approximately 200 species of higher plants have been observed in the lake's environment, which contains the most extensive wetland habitat in the region (Campbell, Poole, Giesen, & Valbo-Jorgensen, 2006; Kummu, Jozsa, Sarkkula, & Koponen, 2014). Gallery forests near the lake's permanent area shoreline provide an important physical barrier between the open lake and floodplain, allowing for sedimentation to occur within the forested zone and preventing it from depositing in the lake's main area (Kummu and Sarkkula, 2008). Prior to human alteration of Tonle Sap's floodplain vegetation, a majority of land cover consisted of closed canopy of small to medium trees. Most of the habitat today consists of scrubland with shrubs, scattered trees and herbaceous vegetation mostly consisting of grass and farmland. Much of the lake's floodplain has been converted from tree canopy to agriculture operations (Campbell et al., 2006).

Several other of the lake's natural, hydrological processes have been studied that are not discussed in detail here but are worth noting. To name a few, these include processes such as seasonal changes in Tonle Sap river floodplain's inundation area and water volume (Siev *et al.*, 2016), 2-dimensional modeling of inundation processes (Hai *et al.*, 2008) and restoration of historical hydrological data of the lake and contributing areas (Inomata and Fukami, 2008). Upstream development impacts on the natural hydrological processes have been greatly studied

and are discussed in a later section of this report. Yet, there are several components of Tonle Sap's hydrologic regime that are still unknown. Groundwater interactions with the floodplain are largely unknown, but it is known that the floodplain plays an important role in recharging the groundwater. A large area of Tonle Sap's watershed is ungauged, even though they provide a significant proportion of flow into the lake. A simple and reliable method for estimating inflows from these tributary systems, as well as rainfall and evaporation over the lake would improve understanding of the lake's overall water balance. Also, overland flow in Tonle Sap River's floodplain is difficult to measure and nearly impossible to quantify accurately. Even though each of these are fundamental components of the system, their impacts on the lake's resources are still largely unknown (Kummu *et al.*, 2014).

2.2 Lake and Air Temperature

Heat is exchanged between the lake surface and air, in and outflowing rivers, and the deeper layer of the water column and sediments. Terms governing surface heat exchange include incident short and long wave solar radiation, reflected short and long wave radiation, back radiation from the water surface, evaporative heat loss and heat conduction. Water quality, solar forcing and cloud cover, air temperature, mixing from wind, flow regimes and lake bathymetry are the main factors that control surface water temperature of a lake at any point in time. Waters deeper in the water column tend to be cooler, as radiation penetration decreases with depth. A lake's surface temperature tends to be homothermal, if wind energy is significant enough to drive mixing (Bengtsson, 2012).

Water temperature regulates many processes in lakes including physical, chemical and biological processes. These processes include reaction and metabolic rates, species distribution, nutrient cycling and the concentration of dissolved gases. As heat goes into a lake system primarily

through the surface and mixes to the bottom, chemical and metabolic reaction rates throughout the water column and interstitial layer are directly impacted. Bacteria, zooplankton, epiphyte, macrophytes and all aquatic vertebrate and invertebrate species are directly dependent upon stable thermal regimes. Growth rates and photorespiration are directly a function of temperature, and increased temperatures observed in lakes around the world have been linked to increased algal production (Wright, Holly, Bradley, & Krajewski, 1999). Increased temperatures have also been linked to a decrease in fish body size (Ilha, Schiesari, Yanagawa, Jankowski, & Navas, 2018). Holtgrieve et al. (2013) modeling study identified a negative correlation between Tonle Sap Lake and its floodplain's metabolic balance (respiration/gross primary productivity, $R^2 = 0.46$), indicating a relationship between Tonle Sap Lake's species metabolism and physical conditions.

Watershed factors that have the most significant impact on the aforementioned parameters and consequently a lake's surface temperature are climate and shading, while dams have a more noticeable impact on their tributaries. Many of these variables are shown in Figure 2.9. Lakes can be valuable tools for water resource managers as they are highly sensitive to changes occurring in their watersheds and their impacts to water resources. Anthropogenic impacts have been studied in hundreds of lakes around the world such as climate change, land and dam development. Adrian et al. (2009) identified various indicators in lakes that act as regional responses to climate change, characteristics of their catchments and changes in lake mixing regimes. This study notes that while lakes are effective sentinels of climate change due to their sensitivity to local climate, they also integrate changes in land-use that can either compound or weaken impacts of climate change. Lake responses to each of these can vary by geographic location, regional climate and land use. As a tropical lake, air temperature is a driving variable of Tonle Sap's water quality characteristics, and surface temperature is the most effective indicator for identifying impacts of climate change. Also,

as a tropical lake, habitat and ecosystem services are directly impacted the most by these changes (Adrian et al., 2009). Water temperature is one of the most important variables affecting the function and distribution of organisms, how they interact, and the function of the overall ecological community (Brown, 2004; Clarke & Gaston, 2006).

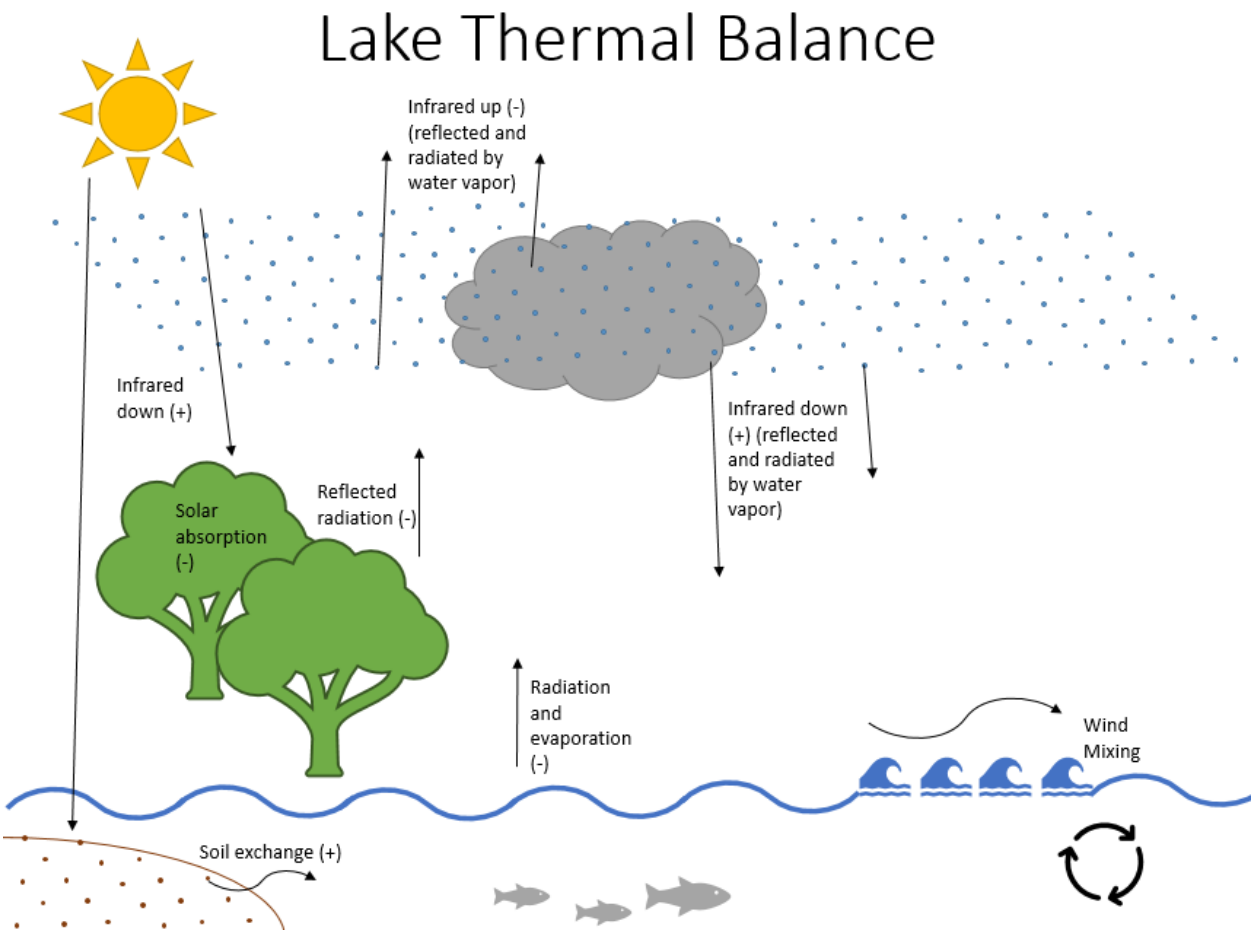

Figure 2.4. Atmospheric and lake thermal energy balance

Manton et al. (2001) identified patterns of warming trends throughout most of Southeast Asia analyzing observed data from 1961 – 1998. Figure 2.10, Figure 2.11, Figure 2.12 and Figure 2.13 summarize their findings on hot days, warm nights and cool night trends. Unfortunately, none of the stations utilizing in this study were located in Cambodia, however, most of the trends are

consistent throughout the Indochina Peninsula. Hot days showed increasing trends during this period throughout most of the region surrounding Cambodia, except for parts of southern Thailand. However, warm nights showed increasing trends while cool nights showed decreasing trends at all stations surrounding the Cambodian region. This study also investigated extreme daily rainfall trends, which showed little statistically significant trends and was more variable spatially. However, the number of rain-days did show significant decrease throughout the Indochina Peninsula, and daily extreme rainfall event frequency showed a significant positive trend.

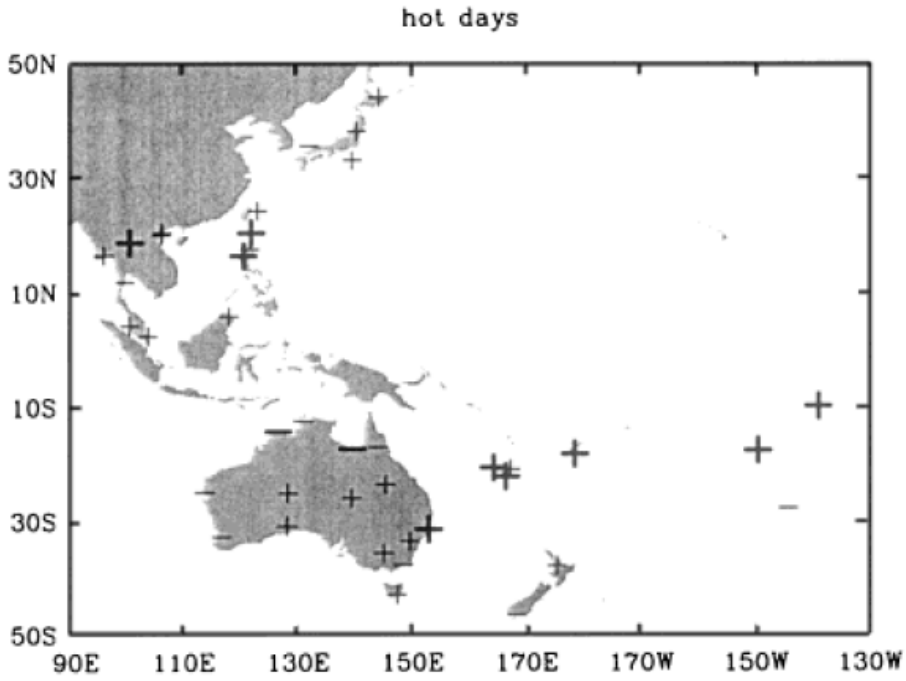

Figure 2.5. Trend in the frequency of days with maximum temperature above the 1961–1990 mean 99th percentile (*hot days*). The sign of the linear trend is indicated by ± symbols at each site; bold indicates significant trends (95%). Data from 1961–1998. (Source: Manton et al., 2001) with permission from Royal Meteorological Society.

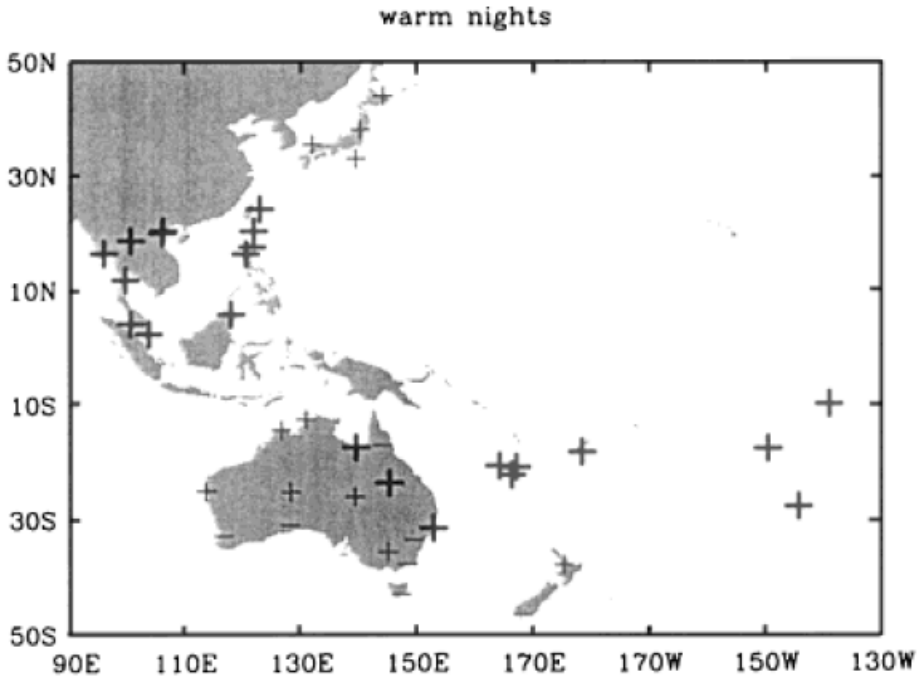

Figure 2.6. Trend in the frequency of days with minimum temperature above the 1961–1990 mean 99th percentile (*warm nights*). The sign of the linear trend is indicated by ± symbols at each site; bold indicates significant trends (95%). Data from 1961–1998 (Source: Manton et al., 2001) with permission from Royal Meteorological Society.

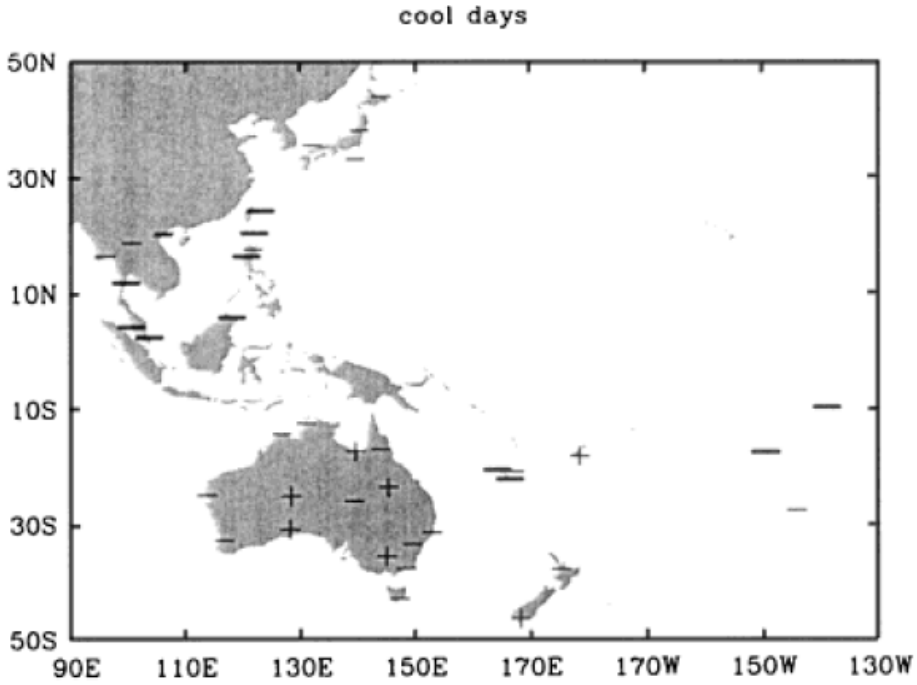

Figure 2.7. Trend in the frequency of days with maximum temperature below the 1961–1990 mean 1st percentile (*cool days*). The sign of the linear trend is indicated by ± symbols at each site; bold indicates significant trends (95%). Data from 1961–1998. (Source: Manton et al., 2001) with permission from Royal Meteorological Society.

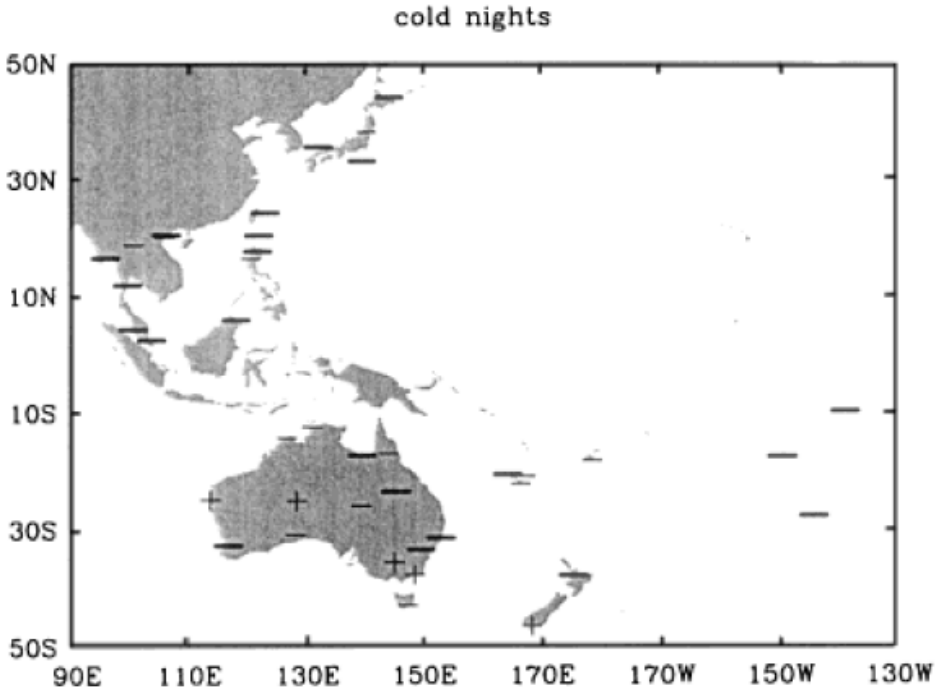

Figure 2.8. Trend in the frequency of days with minimum temperature below the 1961–1990 mean 1st percentile (*cold nights*). The sign of the linear trend is indicated by ± symbols at each site; bold indicates significant trends (95%). Data from 1961–1998. (Source: Manton et al., 2001) with permission from Royal Meteorological Society.

2.3 Land Cover and Land Use

Most of Tonle Sap Lake's floodplain habitat consists of scrubland with shrubs, stunted trees, an occasional scatter taller tree, and herbaceous vegetation dominated by grasses. Submerged are apparently lacking, likely due to the lake's high turbidity and large fluctuation in water level. Local communities utilize much of the floodplain area for real estate (floating villages), agriculture, fish lots, grazing, and wood cutting. Fires have also been found to significantly alter the floodplain's habitat. Less than 10% of the lake's floodplain consists of gallery forests, most of which have been designated as conservation areas by UNESCO and Ramsar (Kummu & Sarkkula, 2008). These forests are usually flooded for about 8 months of the year. Most of the forests that

have existed historically have disappeared, as they have throughout most of the region (Campbell, Poole, Giesen, & Valbo-Jorgensen, 2006). Figure 2.14 describes locations of the floodplain extent, conservation areas and fishing lots, while Figure 2.15 notes the gallery forests in more detail. While agriculture development is growing throughout the floodplain, mapping efforts have been lacking and are currently being studied.

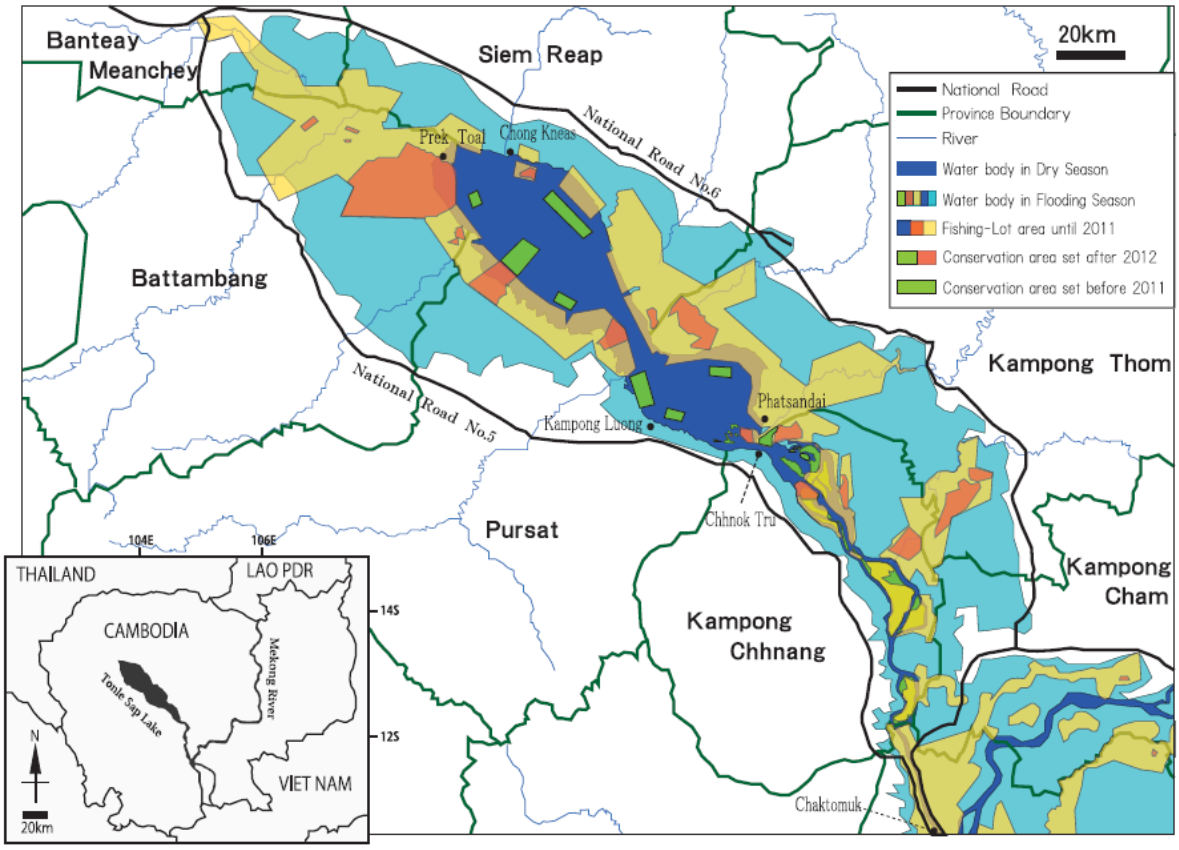

Figure 2.9. Map of Tonle Sap Lake with “fishing-lots” until 2011 and conservation zones based on a map made by the Fisheries Administration Cambodia in 2013. (Source: Ishikawa et al., (2017) with permission from Terra Scientific Publishing Company.

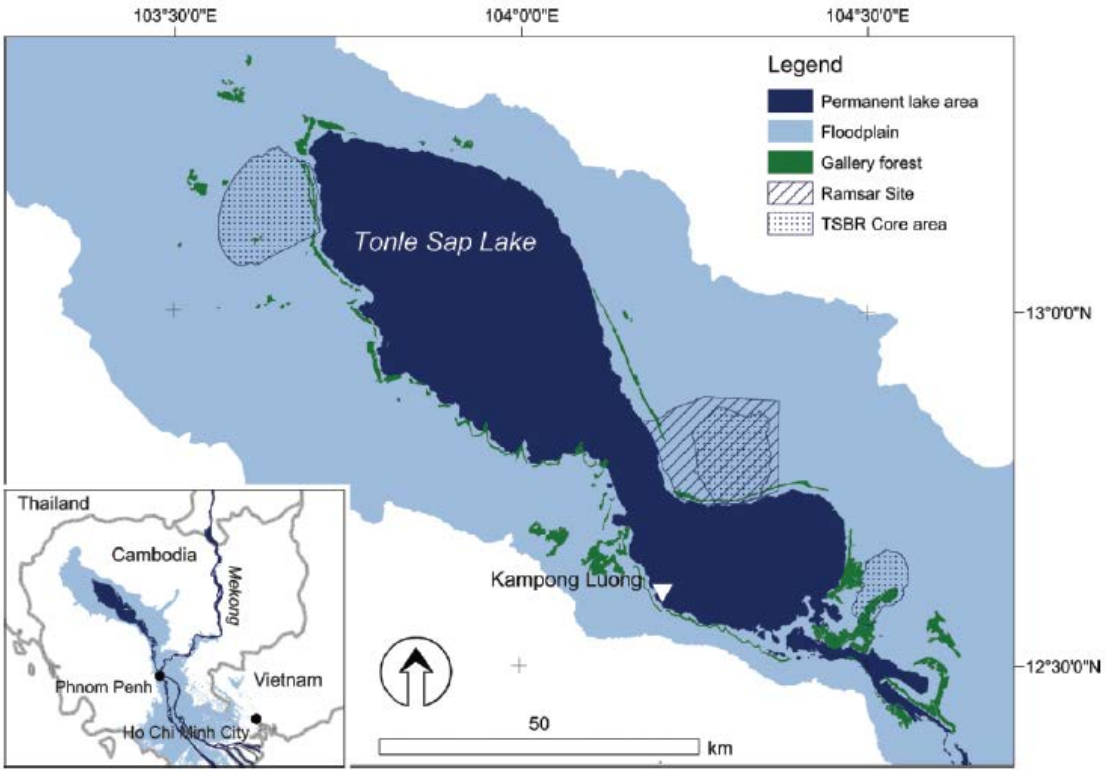

Figure 2.10. Map of Tonle Sap Lake and its location, including the distribution of gallery forest and the protected areas. (Kummu and Sarkkula, 2008) with permission from John Wiley & Sons, Inc.

Land development such as deforestation and agriculture operations have been found to directly impact surface waters all around the world (Brown & Krygier, 1970; Beschta, 1997; Johnson & Jones, 2000; Adrian et al., 2009). Forest cover largely impacts surface waters by intercepting and reflecting incident solar radiation by their leaves, and also by directly impacting air temperature and humidity levels through evapotranspiration (Evans, McGregor, & Petts, 1998; Caissie, 2006). Generally, deforestation has been found to lead to increase surface water temperatures. Silverio et al. (2015) found that deforestation in the Amazon increases mean air temperature by five degrees Celsius, and Macedo et al. (2013) found that deforested areas lead to three to four degree increase in stream mean daily temperature. Agriculture can lead to increased

or decreased runoff temperatures, depending on the local climate and the land use it is replacing. Haddeland et al. found increased irrigation lead to increases in evapotranspiration and lower surface temperatures through a hydrologic modeling study of the Mekong and Colorado River basins (2005). However, while agriculture is increasing in Tonle Sap's watershed, the effects of increased irrigation in conjunction with the major deforestation that is occurring is still unknown.

Areas in Tonle Sap's floodplain, around the permanent lake area that have been highly modified for farming, settlements, logging and burning of forests, population growth, overharvesting of fish and other aquatic species, and illegal fishing. Unstable governance was also identified as a threat to biodiversity management, as management of the lake's resources requires cooperation from a range of government agencies and the local community. There is a general concern that potential changes to sediment deposition put the lake at risk of filling up with sediment, due to upstream deforestation in the watershed. However, further studies concluded that there is no real danger of the main lake area filling up with sediment in the near and mid-range term (Kummu, Penny, Sarkkula, & Koponen, 2008). Invasive species have also been found in Tonle Sap's watershed, however, they appear to be less of a threat than other factors (Campbell, Poole, Giesen, & Valbo-Jorgensen, 2006).

2.4 DAMS

Dams also alter hydrological and thermal regimes in surface water systems (McCully, 2001; Rosenberg, McCully, & Pringle, 2000). Thermal stratification tends to occur more in reservoirs as residence time increases, as stratification occurs as the epilimnion becomes cooler than the hypolimnion over time. As reservoirs behind dams tend to thermally stratify, discharge from a dam can be warmer or cooler than natural temperatures depending on what depth the discharge is released from the reservoir relative to its thermocline.

Development of large-scale irrigation schemes are anticipated to divert significant flow from the Mekong River (Kummu *et al.,* 2014). Between 2003 and 2018, 79 dams totaling in 72 km^3 of volumetric capacity were constructed in the Mekong River Basin (WLE, 2017). While many of the dam operations are unknown, it is unknown whether dams are releasing from the cooler epilimnion or the warmer hypolimnion. Bonnema and Hossain (2017) found the development of hydropower schemes in the Mekong River Basin lead to an increase in residence time to range from 0.9 to 4.04 years. A map of current and future hydropower schemes is shown in Figure 2.16, as described by Bonnema and Hossain (2017). Figure 2.17 shows existing and future cumulative number of dams and storage capacity added to the Mekong River Basin system from dam development.

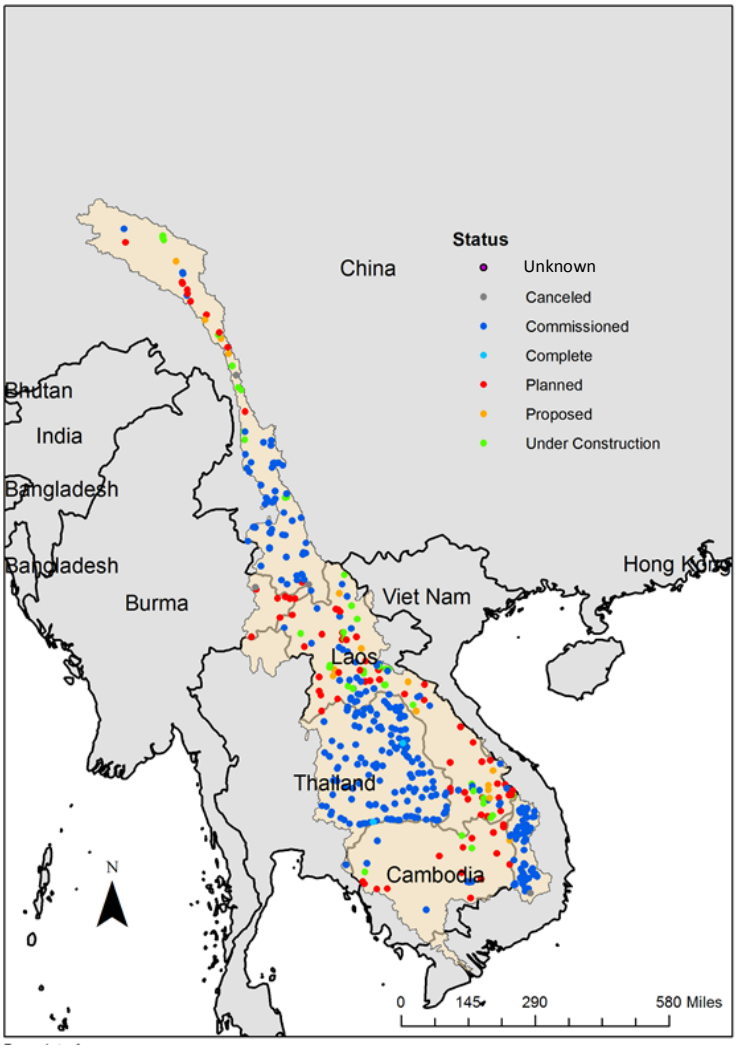

Figure 2.11. Map of Mekong River Basin with current and future dams.

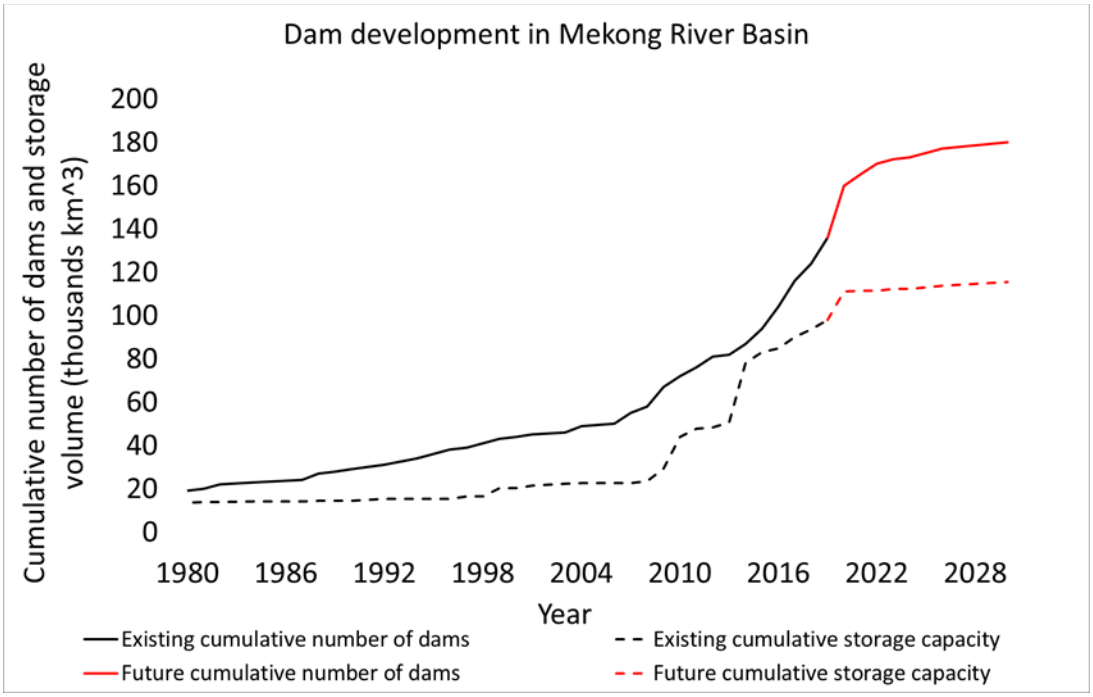

Figure 2.12. Cumulative number of dams and storage behind dams for existing dams (1988 – 2018) and future projected dams (2019 – 2030). (WLE, 2017)

Despite rapid land-cover changes, deforestation and accelerated upstream dam development that began in the 1970's, the Mekong's flow regime was interestingly claimed as essentially natural through 2005 (Kummu and Sarkkula, 2008). The pro-development side often suggests that despite the fact that a majority of the development impact concerns are in China, a ~75% of the Mekong's flow is rainfall driven in the lower basin (Ruiz-Barradas and Nigam, 2018). There are potentially several problems with concluding that dam development in China plays no significant role on impacts in Tonle Sap based on this statistic. First, this statistic that is often cited refers to annual volume, grossly simplifying impacts on intricate flow characteristics that have been altered such as flood-pulse duration, timing, area and water quality characteristics at the Great Lake. Although a majority of the flow originates in the lower basin, impacts on 25% of flow volume in the Mekong (the maximum volume contributed by China's portion of the basin) likely has significant impacts on Tonle Sap's inundation pattern because of the flat nature of its

floodplain. Numerous hydrological impact studies conducted by the MRC, World Bank and several international research labs have concluded that planned development will raise dry season water levels and lower wet season water levels, at varying magnitudes. Several Cumulative Impacts Assessments (CIA) estimated the flood duration would be reduced by 14 days, and the floodplain area, total maximum volume and amplitude would be reduced by 7 – 16% (Osborne, 2006). These CIAs assumed various simplified dam construction, diversion for irrigation and population growth and economic development scenarios, as well as various numerical analysis techniques. Kummu and Sarkkula (2008) applied these estimated changes in a GIS-based analysis to map what these changes in flow regimes mean in terms of Tonle Sap's inundated area, and implications on its gallery forests. The estimated changes in mean water level are shown in Figure 2.5, and Figure 2.18 shows estimates in changes in inundated areas due to increased dry-season water level.

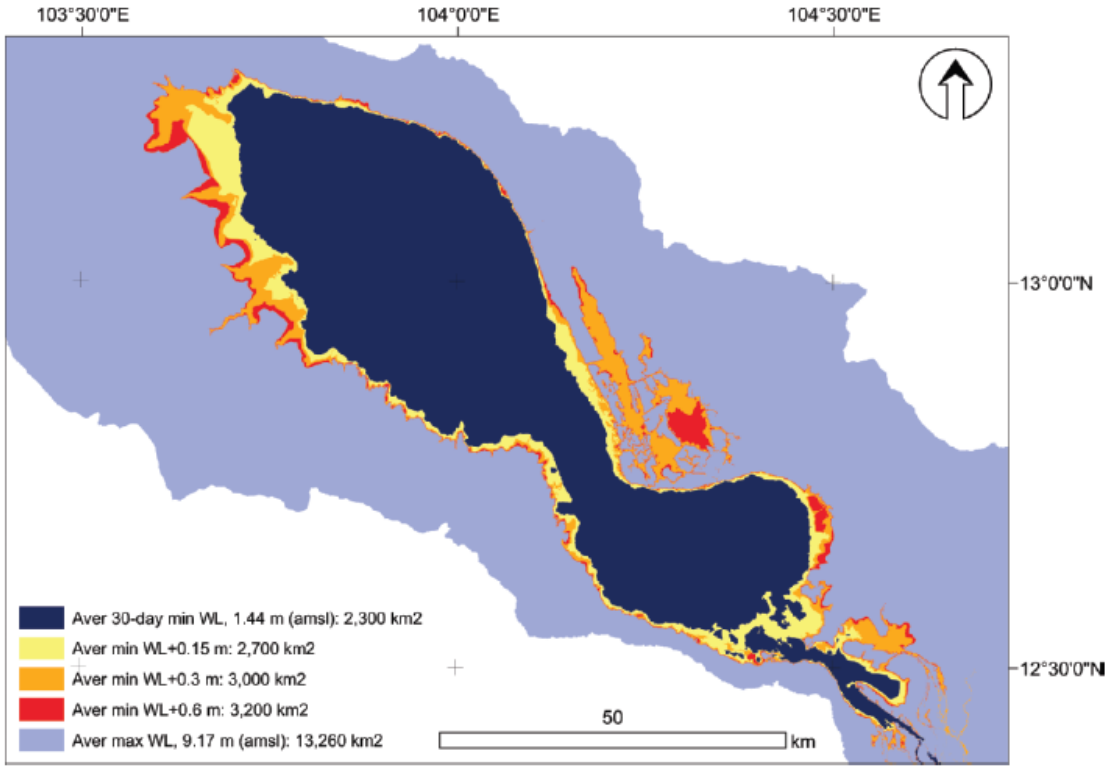

Figure 2.13. Inundated areas due to increased dry season water level (Source: Kummu and Sarkkula, 2008) with permission from John Wiley & Sons, Inc.

2.5 Satellite Remote Sensing of Lake Surface Water Temperature

A common way to investigate lake-surface-water temperature lake water surface temperature (LWST) is by deploying in-situ sensors at in monitoring stations within a system. This approach requires infrastructure and field work to install and maintain the sensors, which can be expensive and time consuming. Also, in-situ temperature sensors cannot adequately capture the spatial heterogeneity of surface temperature across large lake systems. Remote sensing is increasingly utilized for assessment of hydrological and ecological systems, including temperature characteristics. It is particularly useful in regions where in-situ data is unavailable for long-term trend analyses. Remote sensing has been employed extensively in the Mekong River Basin where transboundary and institutional hurdles limit available in-situ data availability. Satellite remote

sensors are also valuable in characterizing spatiotemporal variability of LSWT. Sensors aboard satellites can provide valuable information on hydrological regimes and trends that may be occurring over the past several decades. Schneider and Hook (2010) applied satellite remote sensing thermal infrared imagery in a study of nighttime temperature trends in 167 large inland water bodies around the world from 1985 – 2009. Their results indicate that nighttime temperature has been rapidly warming by an average rate of 0.045°C per year during this period. Warming rates were found to be stronger in water bodies in the mid- and high latitudes than the low-latitudes of the northern hemisphere.

Satellite remote sensors measure at-sensor (also referred to as "top of atmosphere") brightness temperature in the thermal infrared band. Water vapor both absorbs and emits energy in the TIR band, atmospheric corrections must be applied to the sensor data, and only cloud-free pixels can be used for estimating LWST. Brightness temperature and kinetic temperature are highly correlated, and the converted through the Radiative Transfer Equation, shown in Equations 1 through 6.

$$ST = \gamma[\epsilon^{-1}(\varphi_1 L_{sensor} + \varphi_2) + \varphi_3 - L_{sensor}] + T_{sensor} \quad \text{Eqn. 1}$$

Where,

ST = surface temperature (Kelvin)

γ = function

ε = emissivity

ψ_1, ψ_2, ψ_3 = atmospheric functions

and

$$\gamma = \left[\frac{c_2 L_{sensor}}{T_{sensor}^2}\left(\frac{\lambda_{eff}^4}{c_1} L_{sensor} + \lambda_{eff}^{-1}\right)\right]^{-1} \quad \text{Eqn. 2}$$

where,

$c_1 = 1.191x10^8$ Wμm^4/m^2 sr

$c_2 = 1.439x10^4$ Kμm^4

λ_{eff} = effective wavelength of thermal band

and the atmospheric functions are related to atmospheric parameters as:

$$\varphi_1 = \frac{1}{\tau} \quad \text{Eqn. 3}$$

$$\varphi_2 = -L^{down} - \frac{L^{up}}{\tau} \quad \text{Eqn. 4}$$

$$\varphi_3 = L^{down} \quad \text{Eqn. 5}$$

where,

L_{up} = upward emitted radiance (increases with water vapor, atmosphere emits more radiance)

L_{down} = downward emitted radiance (increases with water vapor, atmosphere reflects more radiance)

τ = atmospheric transmittance (decreases with increase in water vapor, which interacts with radiance emitted and reflected by the surface)

Upward emitted radiance increases with increase in water vapor and the atmosphere emits more radiance. Downward emitted radiance also increases with increase in water vapor, as the atmosphere reflects more radiance. Atmospheric transmittance decreases with increase in water vapor, which interacts with radiance emitted and reflected by the surface.

The atmospheric functions are often simplified to:

$$\varphi_n = c_n w^2 + b_n w + a_n \quad \text{Eqn. 6}$$

where,

n = 1,2,3

w = atmospheric water vapor content

a,b,c = satellite sensor and regionally specific empirical coefficients

Various methodologies exist to correct for atmospheric interference as described in the equations above and vary for every satellite sensor and global region. The most common and accurate technique is known as the split-window technique, which compares the difference between two adjacent thermal channels (typically 10.5 – 11.5 μm and 11.5 – 12.5 μm) to account for atmospheric attenuation and derive the surface temperature (Maul & Sidran, 1971). Coefficients of this technique vary from sensor to sensor, as a function of parameters such as spectral response function, emissivity, water vapor in the atmosphere, and View Zenith Angle of the sensor. These coefficients are empirically derived through regression analyses simulated through radiative transfer models like MODTRAN against the atmospheric profiles, and typically vary for global regions. Algorithms developed for ocean surface temperatures are often interchangeable with inland freshwater bodies, however, emissivity does vary based on salinity. Emissivity can vary based on water quality, such as salinity, which can result in errors between 0.2 – 0.5 °C for LWST estimations (Hulley, Hook, & Schneider, 2011; Simon, Tormos, & Danis, 2014). Sensor and lake specific coefficients have been published for numerous global lakes for satellite sensors Moderate Resolution Imaging Spectroradiometer (MODIS) aboard Aqua and Terra satellites, Advanced Very High-Resolution Radiometer AVHRR and Advanced Along Track Scanning Radiometer (AATSR) data (Hulley, Hook, & Schneider, 2011). Satellite-derived surface water temperature reports observations of the "skin-temperature," or approximately the upper 100-micrometers of the top layer of the water column. Because Tonle Sap Lake is relatively shallow (< 10 m) and located in a tropical climate with continuous mixing, little thermal stratification has been observed (Campbell, Poole, Giesen, & Valbo-Jorgensen, 2006). Therefore, the satellite-based surface temperature trend can be considered a reasonable proxy for the lake's depth-averaged thermal characteristic at any given time or location.

Various satellites include thermal infrared sensors, such as the National Oceanic and Atmospheric Administration's (NOAA) (AVHRR) aboard several NOAA satellites, MODIS aboard the Aqua and Terra satellites, Enhanced Thematic Mapper and other sensors aboard various Landsat satellites, to name a few. Tavares et al. (2019) assessed the accuracy of MODIS and Landsat 7 Enhanced Thematic Mapper Plus (ETM+) sensors for the application of estimating LWST of a large subtropical lake located in Brazil. MODIS products MOD11 LST and MOD28 SST products were compared directly with one another. Various methods of estimating LWST from Landsat brightness temperature data were also compared with one another. The first Landsat method applied the radiative transfer equation (RTE) using NASA's Atmospheric Correction Parameter Calculator (AtmCorr) parameters, and the second method implemented single-channel algorithm applying data from various atmospheric model databases. Their results indicate that MOD11 is the most accurate and recommended product for estimated LWST as it obtained the highest accuracy (RMSE of 1.05°C). The AtmCorr method of Landsat-derived LWST obtained the highest accuracy amongst the Landsat methodologies (RMSE 1.07°C, relative to in-situ observations) and was found to show the lowest error in small lakes. This study also notes that Landsat-derived LWST implementing the RTE is highly sensitive to atmospheric parameters and emissivity.

NOAA's AVHRR is commonly used for analyzing long-term temperature trends of lakes (Schneider & Hook, 2010; Pareeth, Salmaso, Adrian, & Neteler, 2016). Orbital drifting effects on land and sea surface temperature observations on the aforementioned NOAA satellite products has been observed (Jin & Treadon, 2003). Orbital drift was designed in the satellite's orbit to avoid direct sunshine on the instruments (Price, 1991). This orbital drift leads to the temperature observations occurring at different local times of day, resulting in inconsistency in the time of

observations. This can greatly affect long-term temperature trend analyses, as surface temperature varies diurnally. A cooling effect is clearly observed when looking at a time series of daytime surface temperature from a single NOAA satellite. Thus, AVHRR's daytime data can only be used if in-situ data is available to calibrate and correct for the orbital drift. Schneider and Hook (2010) demonstrate that using AVHRR's nighttime data minimizes bias due to orbital drift of NOAA's satellites.

The next chapter discusses this study's methodology for quantifying Tonle Sap Lake's long-term temperature trends and watershed impacts to those trends. The study region described was chosen based on information discussed in Chapter 2.1. Various datasets and analyses were conducted based on information discussed in Chapter 2.2 through 2.5 and are described in more detail in the ensuing chapter.

Chapter 3. METHODOLOGY

3.1 STUDY LOCATIONS

Various studies have indicated unique characteristics between the northwest (NW) and southeast (SE) portion of the lake due to the different tributaries located in each of those regions (Oyagi et al., 2017). Water quality data in the SE region tends to be more influenced by the inflow from the Tonle Sap River during high water, while the NW region tends to be influenced by the eleven other tributaries (Yen, et al., 2008). Thus, the NW and SE lake regions were separately analyzed and delineated manually based on locations where there is always water utilizing the Global Surface Water Explorer (Pekel et. al, 2016). The boundaries of each region are at least a distance (in length) of 4-kilometers from the shoreline to ensure temperature data was extracted purely for the lake surface without interference from shoreline pixels. The northwest study region

spans 706 km^2 and the southeast study region spans 226 km^2. Tonle Sap's watershed was delineated according to the HydroSHEDS watershed boundary (Lehner, Verdin, & Jarvis, 2008). Three locations of the size satellite pixels in the Mekong River (MKR) each were included in the water surface temperature analyses to compare trends occurring just upstream to trends occurring within the lake. Three points were selected in each to minimize the bias that might be observed at a single point in each river. These points, as well as the watershed, northwest and southeast lake regions used in this study are shown in Figure 3.1.

Air temperature in Tonle Sap's watershed, just above the lake, and the entire Tonle Sap floodplain region were also included in the analysis. Anthropogenic activities were characterized by annual land cover change in the lake's floodplain and dam development in the Mekong River Basin (discussed in ensuing sections). Each of these were directly compared to Tonle Sap's LWST trends to understand how each parameter's thermal trends correspond to thermal trends in the lake. While other water quality may also influence a lake's thermal characteristics, long-term water quality data is not readily available and was not included in this study.

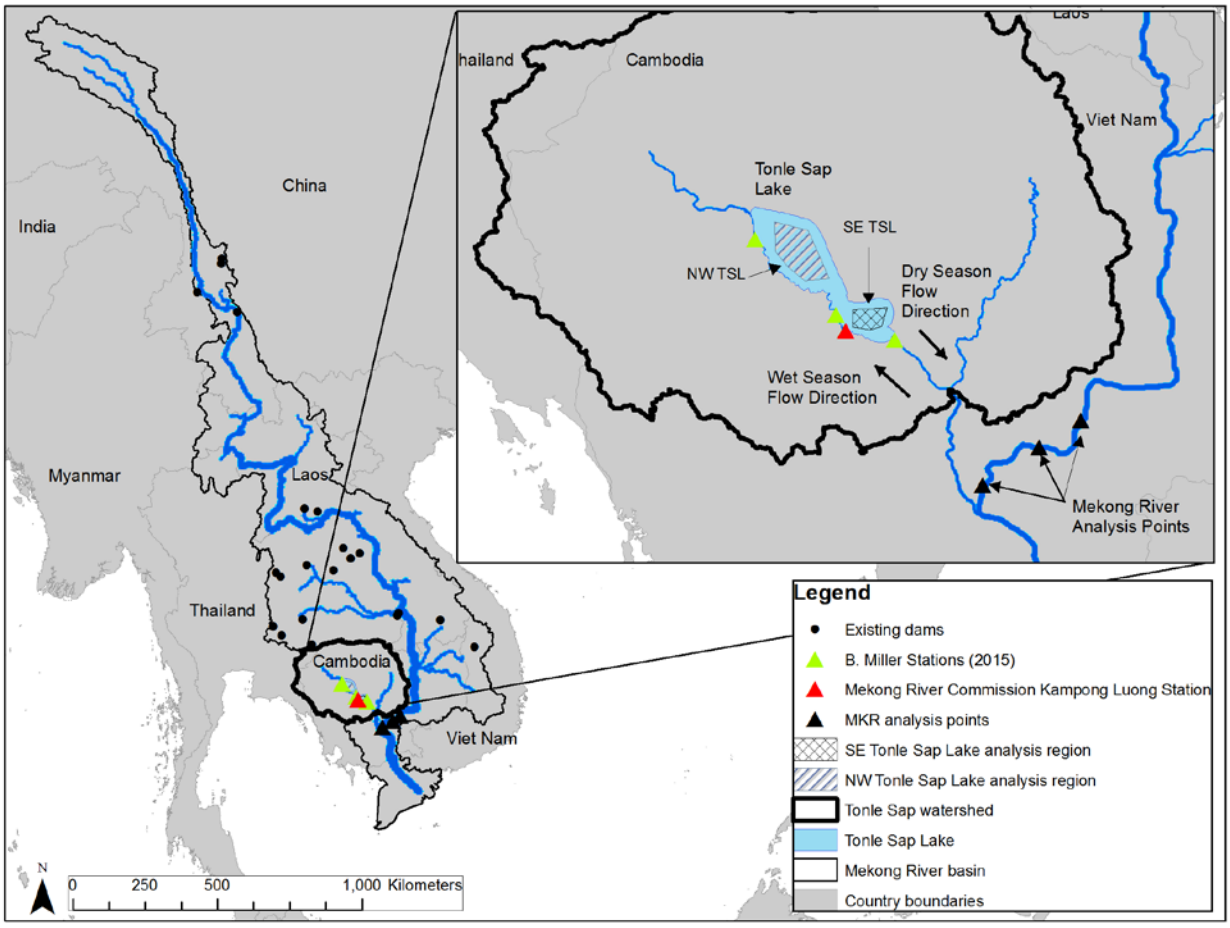

Figure 3.1. Map of the Mekong River Basin, Tonle Sap watershed and lake, existing dam locations and study analysis locations.

3.2 Historical Surface and Air Temperature

Geophysical parameters were directly compared to annual and monthly trends of Tonle Sap Lake's water surface temperature (LWST) to detect the influence of each on the lake's thermal regime. Water surface temperature estimates from multiple satellite products were utilized to determine monthly (dry-season only) long-term and recent trends of temperature, number of warm days/nights and number of cool days/nights per year. For long-term trends, satellite-based NOAA AVHRR Pathfinder Version 5.3 Nighttime Sea Surface Temperature (Pathfinder V5.3) was chosen

as the data is preprocessed converting from at-sensor brightness to surface kinetic temperature. Pathfinder V5.3 data was processed in Google Earth Engine for the available period 1981–2014 at 4-kilometer resolution with a twice-daily repeat (Baker-Yeboah, et al., 2016). Pathfinder V5.3 product combines sensor information aboard the NOAA -7, -9, -11, -14, -16, -17, -18, -19 satellite platforms to collate into a single, twice-daily time series of daytime and nighttime surface temperature. Pathfinder V5.3 collates the data by optimizing different satellites for different time periods to minimize bias that may occur from orbital drift.

Dry-season Pathfinder V5.3 nighttime sea-surface temperature was processed and extracted for the Northwest and Southeast Tonle Sap Lake study regions over the available period except for the period of July 11, 2002 through June 6, 2005 during which observations aboard the NOAA-17 satellite platform are reported, due to significant temporal differences between this satellite and the other aforementioned NOAA satellites. Nighttime data was analyzed, rather than daytime, to further minimize any bias that may occur from orbital drift (Schneider & Hook, 2010). The upstream study locations in the Tonle Sap and Mekong Rivers were excluded from this long-term analysis due to the coarse-spatial resolution of the NOAA AVHRR Pathfinder V5.3 products. In total, 712 number of cloud-free nights were available for the analysis in the NW region, and 323 cloud-free nights in the SE region, removing approximately 5,000 cloudy nights from the analysis. The final time series for NW and SE Pathfinder V5.3 nighttime temperatures are shown in Figure 3.2. On average, the NW and SE regions were found to be very similar in temperature (less than 1 ˚C difference).

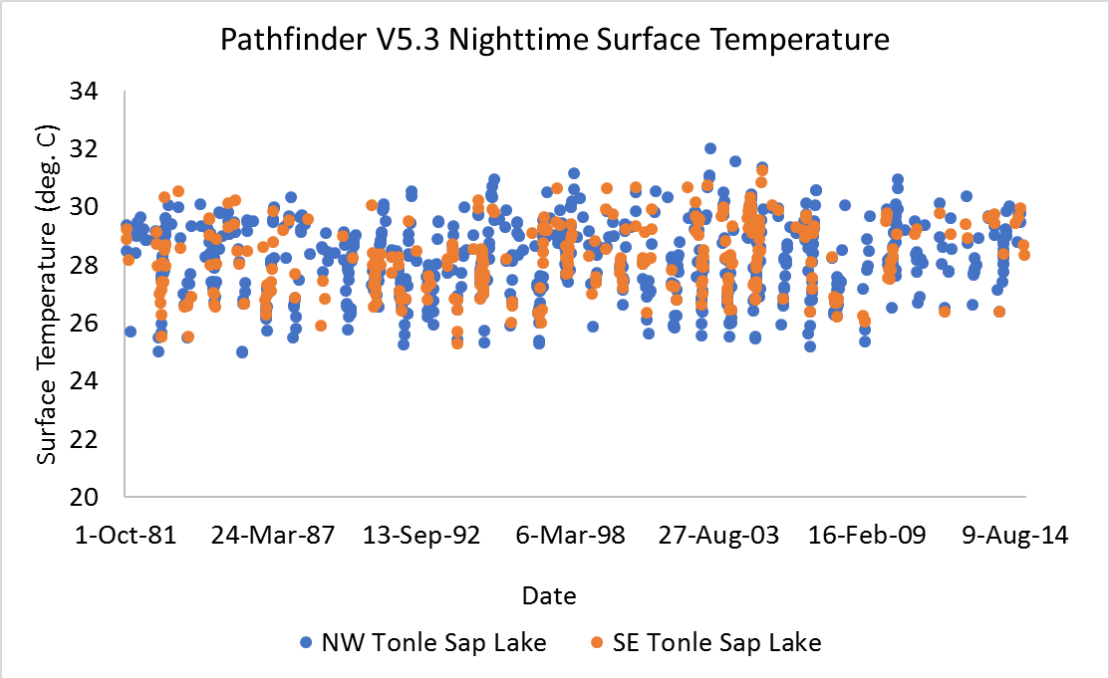

Figure 3.2. Time series of NOAA AVHRR Pathfinder V5.3 nighttime surface temperature for NW and SE Tonle Sap Lake study regions

Cool and warm day and night trends were evaluated for NW and SE Tonle Sap Lake regions, as well as the Mekong River points using MODIS thermal infrared sensor that is on board the Aqua satellite mission. This dataset, also processed in Google Earth Engine, is called the MYD11A1 Version 6 and provides land surface day and nighttime temperature from 2002–2018 at a 1-km resolution (Wan, Hook, & Hulley, 2015). MODIS datasets were analyzed for the cool and warm day and night trends because of its higher frequency of observation (2 per day), while NOAA AVHRR Pathfinder V5.3 data was utilized for analyzing long-term trends because of its longer period of record. Pixels that did not qualify for the clear-sky criteria provided with each product were masked and not included in the analysis (see Chapter 2). The final time series of MODIS LWST is shown in Figure 3.3.

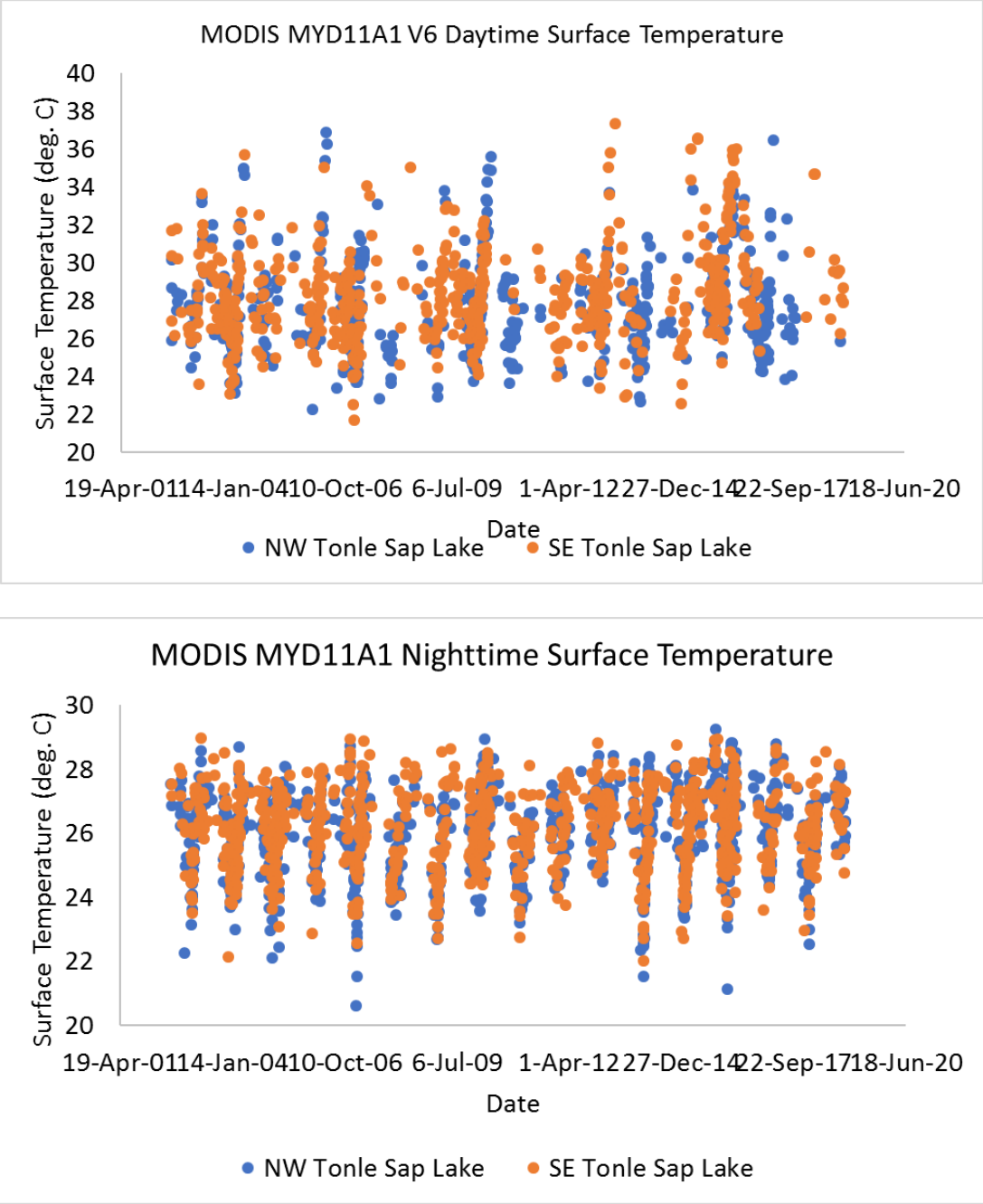

Figure 3.3. Time series of MODIS daytime and nighttime surface temperature for NW and SE Tonle Sap Lake study regions

Air temperature trends were analyzed from the National Centers for Environmental Prediction/National Center for Atmospheric Research (NCEP/NCAR) Reanalysis Project for the same period 1982 – 2018 (Kalnay et al., 1996). The Reanalysis data consists of near-surface (air)

temperature for 2.5 by 2.5 arc degree pixels for a 6-hour cadence, derived from the Climate Data Assimilation System. The Reanalysis system includes a data assimilation of various climate models and observed datasets, spectral statistical interpolation, complex quality control of raw input data, and optimization of averaging several parameters. Input data includes observed data from various countries, however, Cambodia was not listed as one of those countries. Thus, data over Tonle Sap Lake is likely derived from modeling efforts and statistical methods rather than observed data.

Air temperature was analyzed for regions just above the lake surface and floodplain, as well as entire watershed regions to produce two time series of spatially averaged air temperature in Google Earth Engine. Due to the coarse spatial resolution, air temperature was not analyzed for the NW and SW lake regions separately, but the lake as a whole instead. Air temperature was also not analyzed for the Mekong points due to coarse spatial resolution. Annual and monthly temperature trends for the entire watershed and immediate lake and floodplain region were separately compared to both lake areas LWST. Air temperature was averaged over all pixels masked within the study regions. The daytime temperature time series was developed from data with a timestep of noon, and nighttime with a timestep of midnight. Daytime and nighttime air temperature are shown in Figure 3.4.

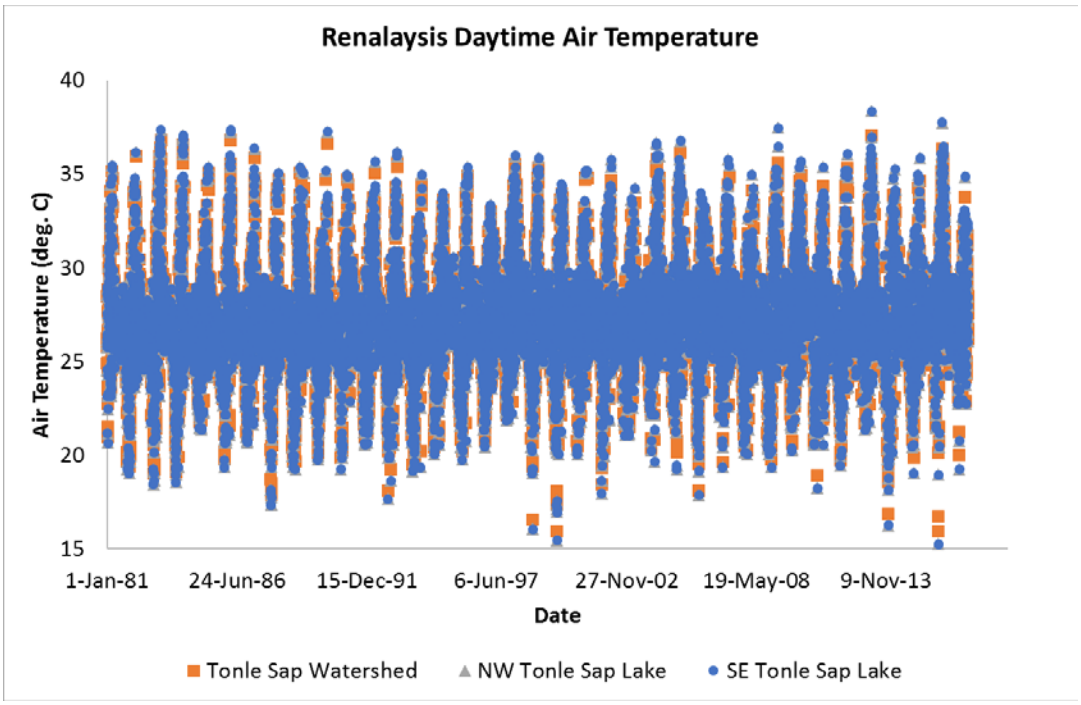

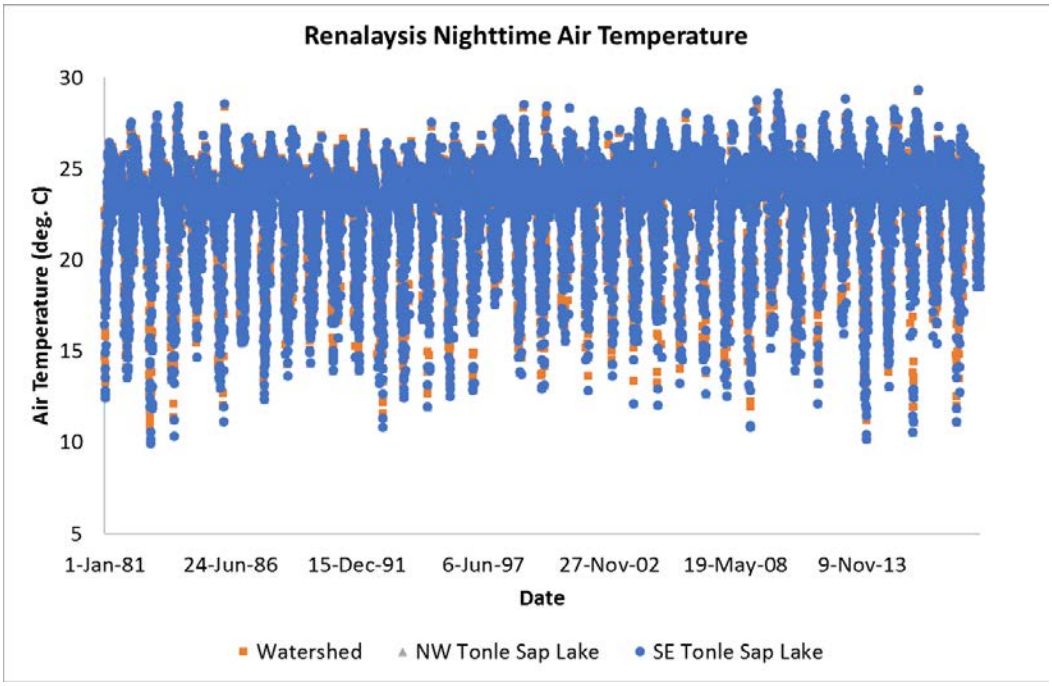

Figure 3.4. Time series of NCEP/NCAR Reanalysis daytime and nighttime air temperature for Tonle Sap Lake watershed and NW and SE Tonle Sap Lake study regions

Temperature data were averaged over pixels masked to each study area to produce an average temperature per day for the Pathfinder V5.3, MODIS and Reanalysis datasets. Any day with over 40% of the pixels masked due to cloud-interference were removed from the analysis to remove bias that may occur in neighboring pixels. For the Mekong River points, only the temperature record of the pixel at each point was extracted. Two additional post-processing steps were executed to discard images that may have been overly skewed by cloud interference. The first was conducted by removing days with more than 40% of the pixels within the study area flagged as clouds. Second, an advanced filter based on inter-quartile range of LWST derived approximately every 16 days, for a lower and upper threshold was applied using equations 1 and 2, respectively (Metz, 2014; Ghent, 2012):

$$Lower\ threshold = 1^{st}\ quartile\ - 1.5\left(3^{rd}\ quartile - 1^{st}\ quartile\right) \quad (1)$$

$$Upper\ threshold = 1^{st}\ quartile\ - 1.5\left(3^{rd}\ quartile + 1^{st}\ quartile\right) \quad (2)$$

The final Pathfinder V5.3 and Reanalysis time series were averaged monthly and annually to analyze the long-term trends. The full work flow for long-term temperature trends is shown in Figure 3.5. The number of warm days was calculated as the number of days that exceeded the long-term monthly average from the MODIS dataset. This same step was carried out with the nighttime time series to calculate the number of warm nights per year. The non-parametric Mann-Kendall test was applied to all temperature time series to identify statistical significance in the presence of monotonic upward or downward trends within a given confidence level. Sen's slope method, which is insensitive to outliers, was utilized for a robust estimation of significant trends (Sen, 1968).

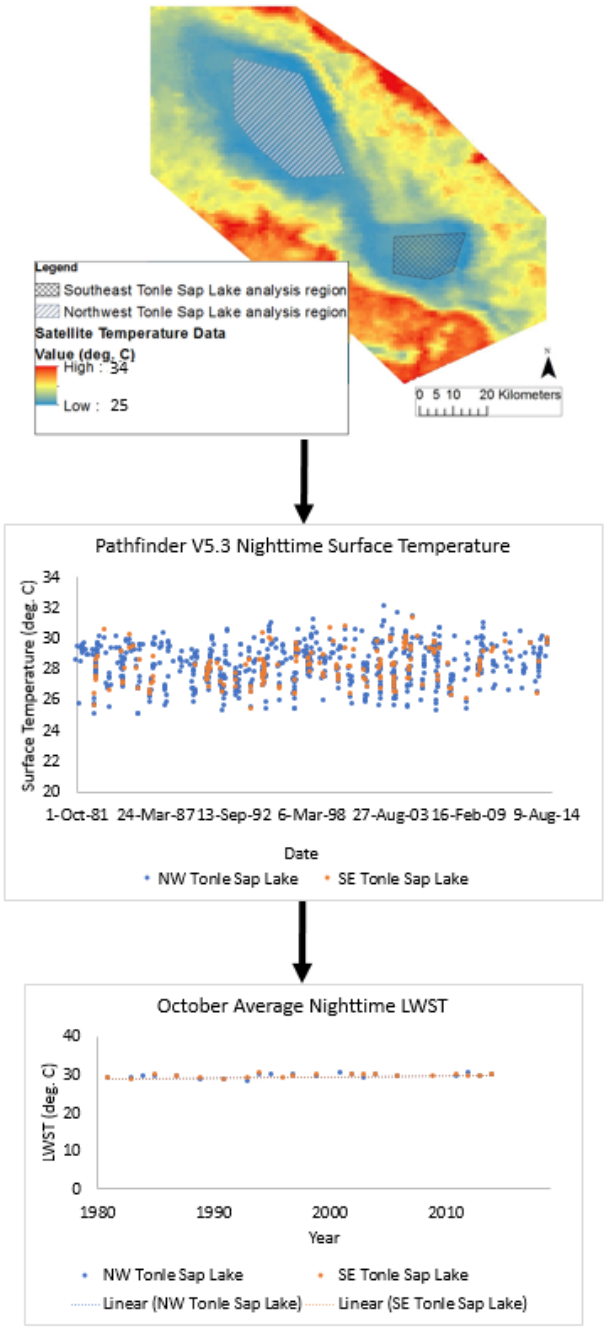

Figure 3.5. Flowchart demonstrating the steps for obtaining Pathfinder V5.3 LWST satellite remote sensing data and calculating long-term trends of monthly average LWST. Note, data shown is brightness temperature derived from Landsat products. All units are in degrees Celsius.

The single-channel algorithm method described in Section 2.5 was analyzed for applying Landsat top-of-atmosphere brightness temperature products for potential application in the long-term surface temperature trend analysis. Methods applying various atmospheric sounding databases described by Jiménez-Muñoz et al. (2009) were attempted for Landsat 5 Band 6 observations. The atmospheric sounding databases applied included STD66, TIGR61, TIGR1761, TIGR2311, and SAFREE402. Each of these resulted in -5 – 7 ˚C difference from MODIS. Ultimately, none of the results matched in-situ nor MODIS (which closely matches in-situ data) well. Thus, it was decided not to utilize Landsat products for this particular study. Further investigation of other methods, particularly the application of NASA's AtmCorr data recommended by Tavares et al. (2019) may be an area of further study for temperature trends in Tonle Sap Lake region.

3.3 HISTORICAL LAND COVER

Land cover data was retrieved from the International Geosphere-Biosphere Programme (IGBP) supervised land cover classification of MODIS Aqua and Terra reflectance data (Friedl & Sulla-Menashe, 2015). One land cover type is included for each pixel at 500-meter spatial resolution and one-year interval. Land cover change was determined for each year by calculating the change in total area of each land cover classification type. Relevant land cover types were grouped into two categories. The "forested" area category summed up the areas whose pixels were categorized as "evergreen broadleaf forests," "deciduous broadleaf forests," "mixed forests" and "woody savannas." The "agriculture" category summed up the areas of pixels that were categorized as "croplands" and "cropland/natural vegetation mosaics." These classes are adequate to capture the influence of species diversity that exists in the lake's floodplain, as described by

Campbell et al. (2006). Only the area in the lake's approximated floodplain area were included in the land cover analysis, spanning 17,300 km^2.

Land cover over Tonle Sap Lake's watershed is shown in Table 3.1 for years 2001 through 2017. As can be observed in Figure 3.6, much of the lake's floodplain area was forested in 2001 (green pixels shown in floodplain), and most of this area was converted to the "savannas" category by 2017. Further investigation into true color composite of Landsat 8 imagery showed agriculture operations were sometimes inaccurately classified as grassland and permanent wetlands. This is particularly true for operations closer to the lake that are inundated during the Monsoon season. This can be observed in Figure 3.7, which shows areas classified as savanna and woody savanna in the IGBP data (Figure 3.7a), where the Landsat imagery (Figure 3.7b) clearly shows agriculture operations. This area's land cover changes throughout the year from water during the monsoon season to agriculture and other vegetative land cover during the dry season, so the annual IGBP data is oversimplified temporally as well. Thus, it should be noted that agriculture operations are likely underestimated in this study. This error is also noted in the IGBP's documentation (Friedl & Sulla-Menashe, 2015).

Table 3.1. IGBP results for land cover in Tonle Sap Lake's Floodplain. All units are in square-kilometers.

Year	Evergreen Needleleaf Forests	Evergreen Broadleaf Forests	Deciduous Needleleaf Forests	Deciduous Broadleaf Forests	Mixed Forests	Closed Shrublands	Open Shrubland	Woody Savannas	Savannas	Grasslands	Permanent Wetlands	Croplands	Urban and Built-up Lands	Cropland/Natural Vegetation Mosaics	Permanent Snow and Ice	Barren	Water Bodies
2001	-	3,279	-	91	1	1	-	1,393	527	4,547	1,281	3,456	28	29	-	0	2,682
2002	-	3,143	-	106	2	1	-	1,401	549	4,633	1,194	3,548	28	30	-	0	2,682
2003	-	2,738	-	114	4	0	-	1,573	634	4,739	1,132	3,649	28	28	-	0	2,676
2004	-	2,480	-	138	5	-	-	1,659	688	4,805	1,097	3,720	28	26	-	0	2,669
2005	-	2,282	-	163	4	-	-	1,750	733	4,821	1,083	3,756	28	27	-	0	2,668
2006	-	2,155	-	161	4	-	-	1,836	785	4,857	1,065	3,731	29	23	-	0	2,669
2007	-	1,884	-	147	4	-	-	2,032	838	4,925	1,065	3,698	29	24	-	0	2,668
2008	-	1,701	-	136	3	-	-	2,173	853	5,002	1,060	3,670	29	22	-	0	2,667
2009	-	1,476	-	124	2	0	-	2,321	861	5,065	1,060	3,686	29	26	-	0	2,666
2010	-	1,231	-	100	1	0	-	2,524	862	5,085	1,060	3,736	30	28	-	0	2,658
2011	-	1,157	-	103	1	0	-	2,552	816	5,181	1,071	3,719	30	30	-	0	2,656
2012	-	1,039	-	89	0	1	-	2,644	813	5,174	1,078	3,760	30	35	-	0	2,653
2013	-	879	-	86	-	0	-	2,763	796	5,203	1,083	3,795	30	39	-	0	2,641
2014	-	769	-	82	-	0	-	2,801	834	5,145	1,081	3,894	30	42	-	0	2,637
2015	-	592	-	72	-	0	-	2,864	919	5,108	1,078	3,977	31	45	-	0	2,630
2016	-	470	-	76	0	1	-	2,811	918	5,181	1,116	4,040	31	43	-	0	2,629
2017	-	478	-	126	1	-	-	2,600	847	5,496	1,176	3,875	32	47	-	0	2,637

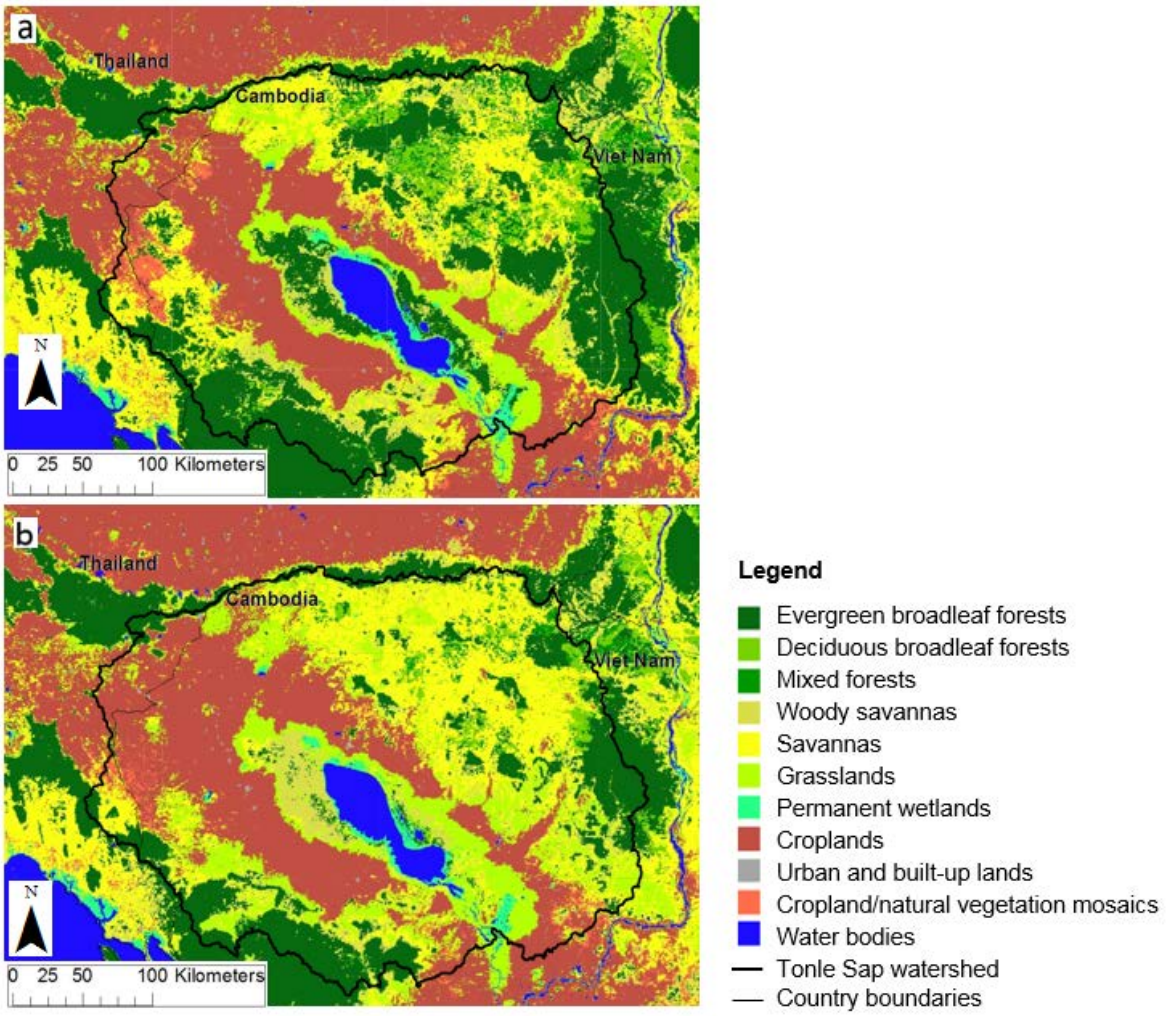

Figure 3.6. Map of the land cover in Tonle Sap watershed for a) the year 2001 and b) the year 2017

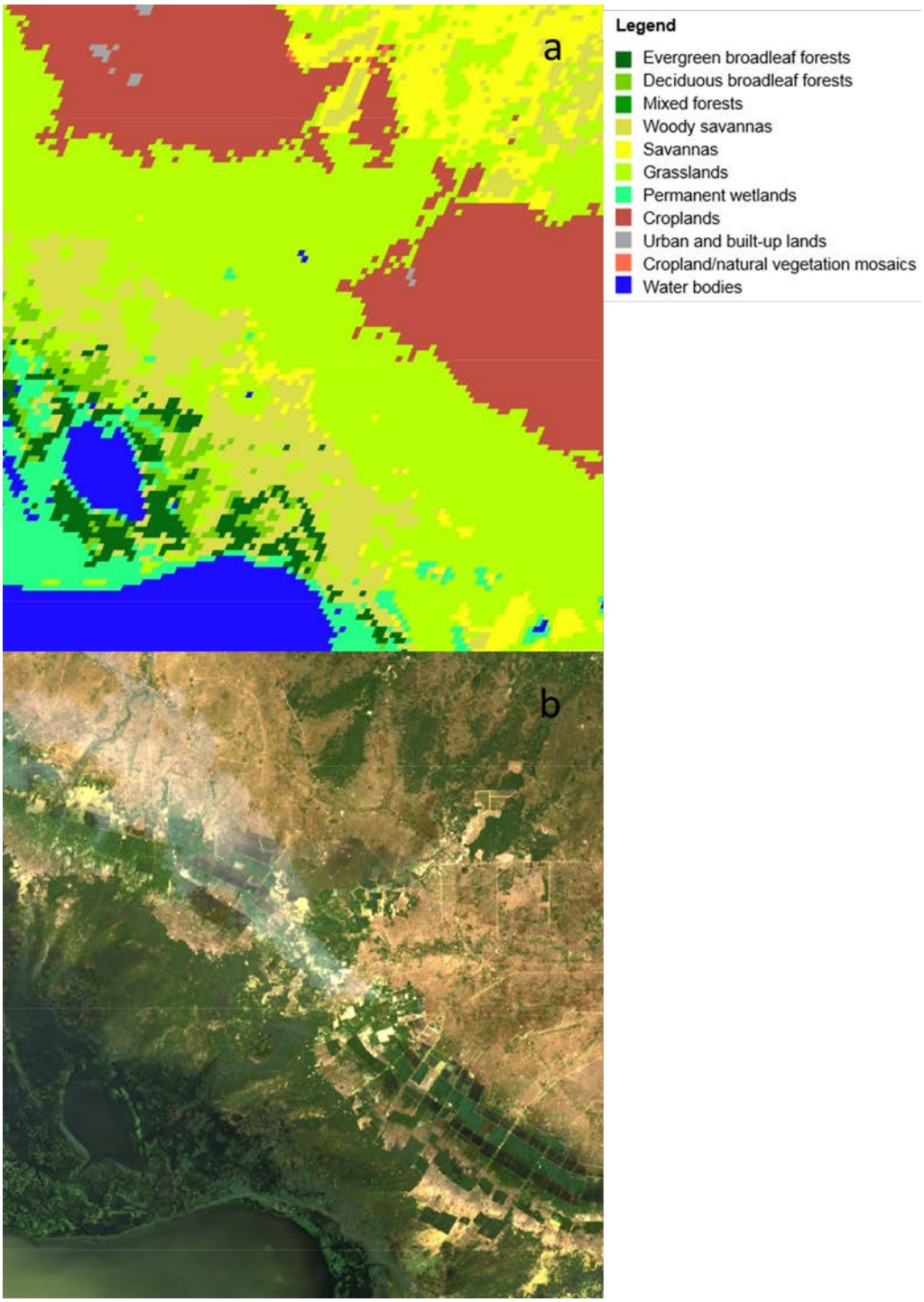

Figure 3.7. a) Map of the IGBP land cover classification in Tonle Sap floodplain and b) Landsat 8 true color composite over the same region for the year 2017

3.4 DAM DEVELOPMENT

Tonle Sap's LWST trends were compared directly with the construction of numerous dams in the Mekong River Basin. The rate of increase in the number of dams and storage volume per year for the Mekong River Basin was derived utilizing the dataset CGIAR Research Program's Dataset on the Dams of the Mekong (2017). The dataset includes a comprehensive list of dams that have been constructed from 1956 through the end of the analysis period. All dams located within the Mekong River basin were incorporated into the analysis to derive the cumulative number of dams constructed and storage added to the river system for each year. A map of existing dams is shown in Figure 2.16, and the cumulative number of dams and volume is shown in Figure 2.17. These trends were compared to annual trends in warm days and nights to determine if dam development trends corresponded to any warming or cooling trends seen in Tonle Sap LWST, as well as in Tonle Sap and Mekong River surface temperature. Further details on the dam data is provided in Appendix A.

The next chapter discusses the results of Tonle Sap Lake's long-term temperature trends and impacts to those trends from land cover changes and dam development, based on methodologies outlined in this chapter.

Chapter 4. RESULTS

4.1 Satellite Remote Sensing Data Lake Water Surface Temperature Validation

Numerous lakes have permanently-deployed buoys to monitor lake temperature, however, this data does not exist for Tonle Sap Lake. No direct validation of the satellite surface temperature datasets was possible due to the lack of long-term in-situ surface temperature measurements. However, two in-situ datasets collected by B. Miller (2015) and the Mekong River Commission's (MRC) (2011) Kampong Luong sampling site (Station ID H02106) were available for various depths and points across the lake. In-situ data locations are shown in Figure 4.1. The in-situ data differs from the remote sensing data temporally and spatially, thus they are not directly comparable. The satellite remote sensing data was compared against the in-situ data to verify it was within a reasonable range of the in-situ data. Although the time of day was not reported for all profiles measured, for profiles that the time was reported occurred between 8 A.M. and 3 P.M. local time. Table 4.1 shows each in-situ observation and which satellite sensor was compared to each station.

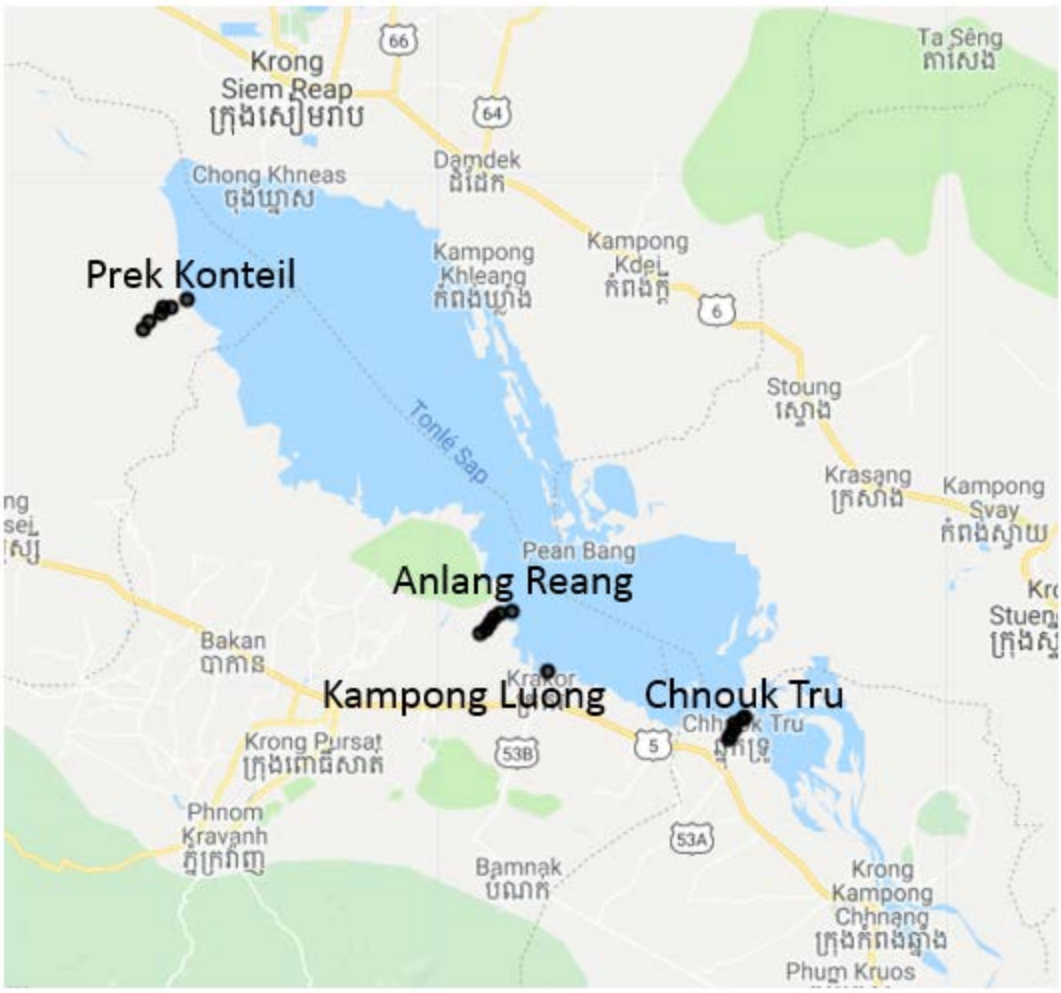

Figure 4.1. Map of the in-situ data observation locations. Prek Konteil, Anland Reang and Chnouk Tru all include 6 observation locations (Miller, 2015). Kampong Luong only has one location (MRC, 2011)

Table 4.2. In-Situ Data Locations and Information, and Satellites Available for Comparison

Station	Source	Date Range	Shallowest Depth Measured (meters)	Satellite Comparison
Prek Konteil	Miller (2015)	11/5/2015 - 11/6/2015	0.214	MODIS AQUA
Anlang Reang	Miller (2015)	10/4/2015	0.244	MODIS AQUA
Chnouk Tru	Miller (2015)	10/27/2015 - 10/28/2015	0.192	MODIS AQUA
Kampong Luong	MRC	2/21/2010 - 12/27/2011	0.5	MODIS AQUAA & NOAA AVHRR

Temperatures from the 2015 dataset ranged between 27.9 °C and 31.8 °C, while the MRC dataset ranged from 25.8 °C to 32.2 °C. The 2015 dataset included temperature profiles for three locations in the lake including one near the NW region at Prek Konteil, near the middle portion of the permanent lake area in Anlang Reang, and the third was located near the SE region at Chnouk Tru. Approximately six samples were collected at each of the three locations between October 4th and November 6th, 2015. All of the temperature profiles are relatively constant from near surface up to 6 meters depth, varying by 1.4 °C over 2-meters at most. The consistency between near surface and deeper temperatures verifies that surface temperature is a sufficient proxy of thermal characteristics throughout Tonle Sap Lake. The 2011 dataset included 12 temperature samples between February 2010 and February 2011. The samples were measured at Kampong Luong at a 0.5-meter depth.

The MODIS satellite temperature data varied from the in-situ datasets by 0.40°C on average. The minimum difference was -2.98 °C at the Chnouk Tru station. This in-situ data point was measured 1.5 hours prior to the MODIS satellite observation and at a depth of 0.2 meters. This

particular temperature profile exhibited a relatively strong thermocline with a difference between the near surface and the deepest measurement of 1.2 °C. The maximum difference was 2.02 °C also at Chnouk Tru (Figure 4.1). This in-situ observation was made 2.5 hours before the MODIS satellite observation. The Chnouk Tru station performed relatively worse than the Prek Konteil station (Figure 4.1), which saw a maximum and minimum difference of 0.74 °C and -0.47 °C, relatively. The average MODIS LWST of the NW TSL Study region during the day the Miller (2015) in-situ stations were measured was found to be 29.13 °C, closely matching the 29.51 °C measured by Miller (2015) at nearly the same time of day. Also, the average MODIS LWST of the SE TSL Study region during the day the Miller (2015) in-situ stations were measured was found to be 28.17 °C, which is a bit lower than the 31.21 °C measured by Miller (2015) 2.5 hours prior, but closely matches the 29.19 °C measured by Miller (2015) 3.5 hours prior.

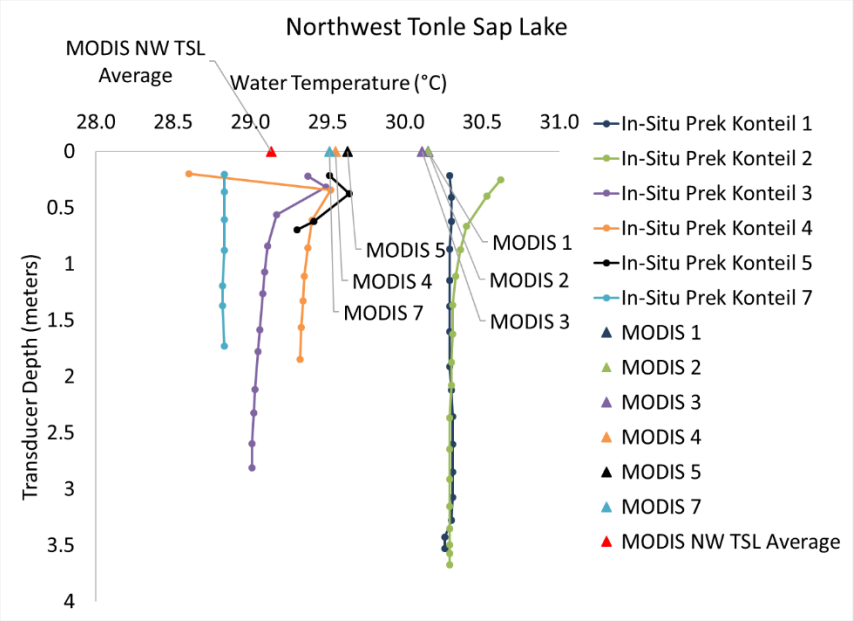

Figure 4.2. Temperature profiles measured at Prek Konteil and MODIS surface temperature measured at same locations

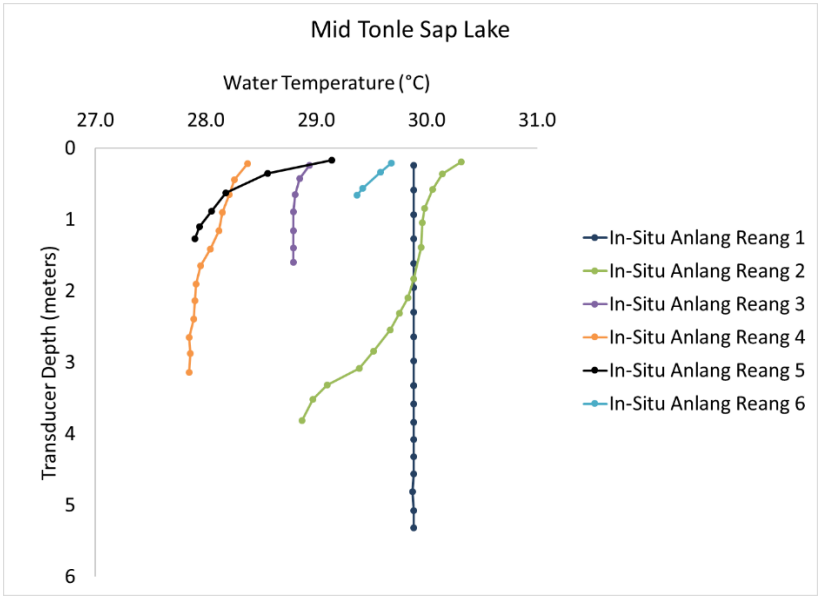

Figure 4.3. Temperature profiles measured at Anlang Reang and MODIS surface temperature measured at same locations

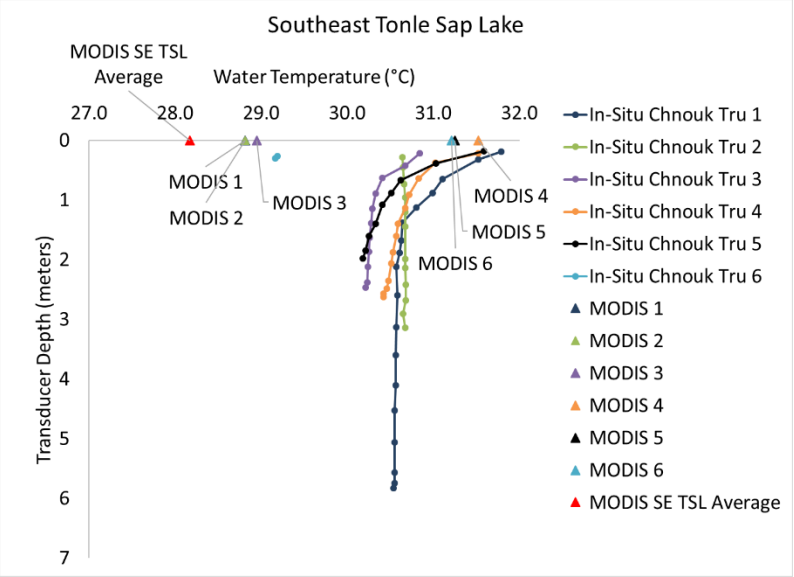

Figure 4.4. Temperature profiles measured at Chnouk Tru and MODIS surface temperature measured at same locations

NOAA AVHRR Pathfinder V5.3 was not compared to the Miller (2015) in-situ data because these satellites were decommissioned by 2014, while the Miller in-situ data was observed in 2015. However, AVHRR and MODIS were compared to another dataset at Kampong Luong provided by MRC (2011). Only six days were available to compare the MRC in-situ data to both satellites. Several days where there was in-situ data, the satellite data shows cloud interference, thus not all days were comparable. The comparison of the Kampong Luong in-situ station to the two satellite products are shown in Figure 4.5 and Table 4.2. Satellite remotely sensed points that deviated the most from in-situ had either a masked pixel in MODIS or AVHRR, indicating cloud-interference is likely the culprit of the relatively large error. The MODIS satellite product does not perform as well against the MRC dataset as it does against the Miller (2015) dataset. However, both satellites perform reasonably well considering several unknowns within the MRC in-situ data. These unknowns include time of day and reliability of sensor. The MRC in-situ data is also

measured at a lower depth than the Miller (2015) stations, and closer to the shore where the thermocline is likely more apparent. On average, MODIS performs better than AVHRR.

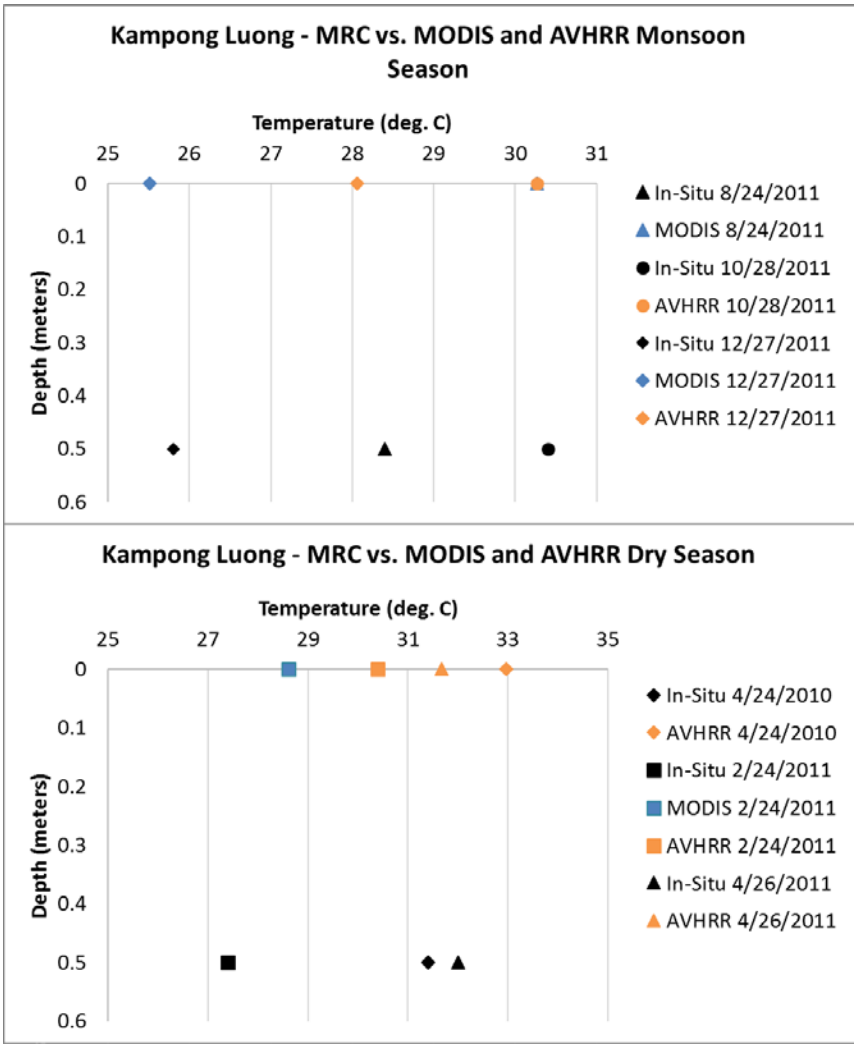

Figure 4.5. Temperature measured at Kampong Luong and MODIS and AVHRR Pathfinder V5.3 surface temperature measured at same locations. Not all days measured at Kampong Luong could be compared to satellite observations due to cloud interference on those days

Table 4.3. In-Situ Data Locations and Information, and Satellites Available for Comparison

Date	In-Situ (˚C)	Modis LWST (˚C)	AVHRR LWST (˚C)	MODIS minus In-Situ	AVHRR minus In-Situ
4/24/2010*	31.4	masked	32.97	-	1.57
6/26/2010	32.2	masked	33.47	-	1.27
2/24/2011*	27.4	28.61	30.39	1.21	2.99
4/26/2011*	32	masked	31.67	-	-0.33
8/24/2011	28.4	30.27	masked	1.87	-
10/28/2011	30.4	masked	30.27	-	-0.13
*Dry season			Average	0.93	1.27

Overall, the satellite remotely sensed data falls within a reasonable range of the in-situ measurements. As the satellite remotely sensed data is measured as brightness temperature and converted to kinetic temperature, various parameters in the conversion can carry various levels of uncertainty. Emissivity values can range from 0.97 to 0.99 for water, mostly depending on salinity. This range can cause an error between 0.2 – 0.5 °C. Many of the MODIS datapoints fell within that range, and a couple of the AVHRR datapoints fell within that range. The satellite remotely sensed data deviated from in-situ data by less than 2 - 3 °C maximum and 1 °C on average, which is reasonable considering the two data sources were measured at different times of day and depths.

4.2 Long-term Recent Temperature Trends

Dry-season monthly mean nighttime surface temperature trends were computed for NW and SE Tonle Sap LWST, and lake and watershed air temperature for the period 1981 – 2014 from Pathfinder V5.3. All wet-season months are not included due to insufficient satellite remote sensing data as a result of cloud interference. During the dry season months, the flow direction in

Tonle Sap River discharges water from Tonle Sap Lake to the Mekong River. Including the Mekong River upstream of the Tonle Sap River confluence in the temperature trend analyses provides insight into whether trends observed in the lake are also occurring in nearby regional surface waters, or if they are unique to the lake. However, Pathfinder V5.3 pixels are too large to obtain data from solely within the rivers without bias from land along the riverbanks. Thus, the river analyses points are not included in the long-term recent temperature trends. Figure 4.6 directly compares the lake's trends, as well as the monthly average water level observed at the Kampong Luong station to provide seasonal context for temperature trends. Air temperature trends averaged over the entire watershed were found to be approximately equal to the SE and NW trends shown in Figure 4.6. All months and regions show warming trends, except for SE Tonle Sap Lake in January and NW Tonle Sap Lake in March shows a slight negative trend. The dry-season LWST trend for both regions indicates warming at an average rate (Sen's slope) of 0.02°C yr^{-1}. The LWST Sen's slope warming trends range from -0.01°C yr^{-1} to 0.06°C yr^{-1} for the NW and SE regions. Two points show cooling trends, which may be due to noise in the raw data.

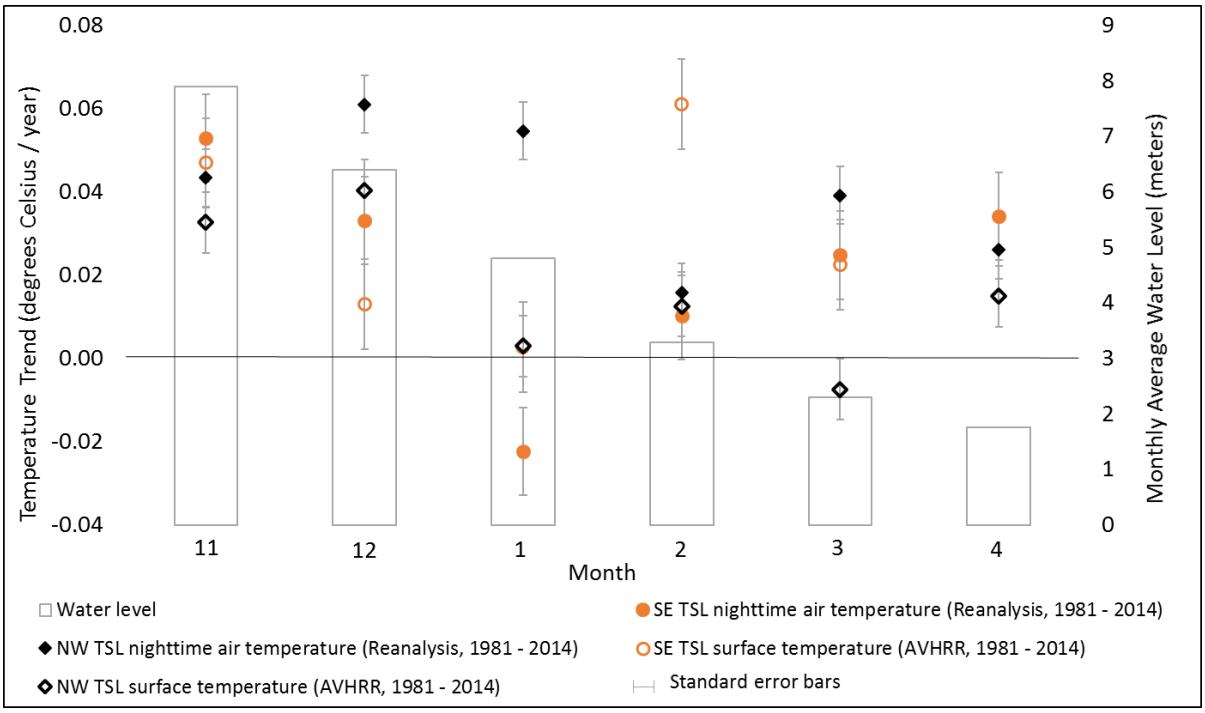

Figure 4.6. Long-term monthly temperature trends for SE and NW Tonle Sap Lake air (Reanalysis) and water surface (NOAA AVHRR Pathfinder V5.3) temperature. Standard error bars shown for all trends. Water level is expressed as elevation above mean sea level in Hatien, Vietnam.

Air temperature over the NW and SE lake regions range between -0.02°C yr^{-1} to 0.06°C yr^{-1}. Air temperature trends between November and March showed statistical significance with *P* ranging between 0.01 and 0.05. LWST showed stronger statistical significance in the SE Tonle Sap Lake region, varying between $P = 0.01$ and $P = 0.05$. The long-term trend analysis revealed that warming or cooling trends are generally consistent amongst both regions analyzed, and relatively consistent between air and surface water temperatures. This indicates that the local surface water temperature trends are likely linked to the warming trends in local air temperature. Thus, drivers of change in the region's air temperature, such as human induced global warming, may be impacting the local surface water temperature trends. Interestingly, the warming trends

tend to weaken with the seasonal decline in water level from November through January but strengthen again in March and April.

Table 4.3 also shows monthly average temperatures for the NW and SE Tonle Sap Lake regions during the dry season months only. Figure 4.7 also provides a visualization of the MODIS LWST results for the years 2003 and 2015. MODIS LWST was used for Table 4.3 and Figure 4.7, as it most closely matched the in-situ data described above. NW and SE Tonle Sap Lake's average dry-season monthly temperature is shown in Table 4.3. The LWST of Tonle Sap Lake can vary from one area to another by as much as 5 °C, however, on average they are well mixed during the dry season (Table 4.3). However, the NW region was found to be cooler than the SE region slightly more often, likely because of the cooler tributaries being the dominate water quality driver during this season which are located in the NW region. The LWST typically varies throughout the dry season by approximately 24-32 °C.

Table 4.4. Monthly Average Tonle Sap Lake Water Surface Temperature for NW and SE Study Regions (2002 through 2018)

Location	October	November	December	January	February	March	April
NW Tonle Sap Lake	27.4	27.1	26.1	26	27.6	30.6	33.3
SE Tonle Sap Lake	28.0	27.4	26.2	26.3	27.9	30.1	33.1

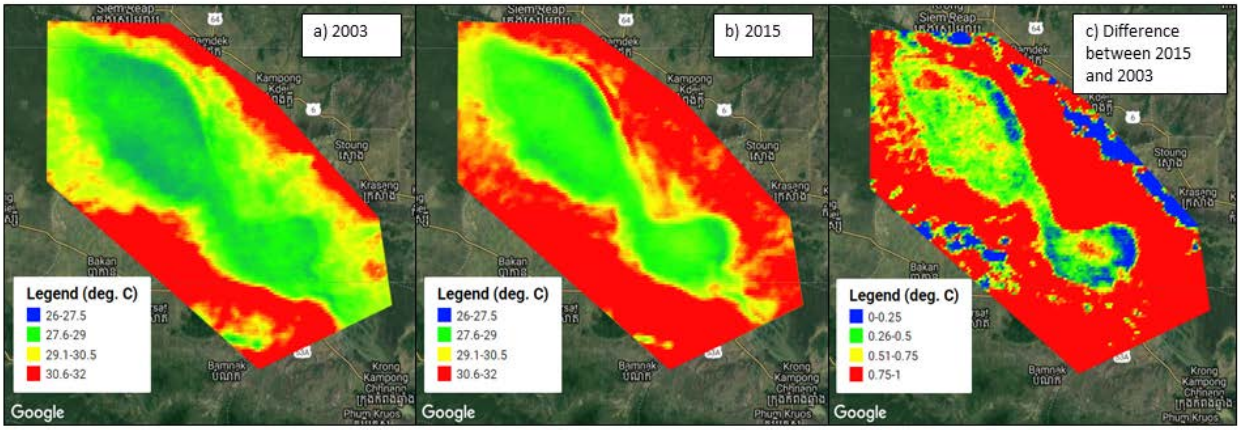

Figure 4.7. Map of the MODIS daytime surface temperature for a) annual average of 2003 (a relatively cool year), b) annual average of 2015 (a relatively warm year) and c) the difference between both images. Units in legend are degrees Celsius.

4.3 Watershed Impacts on Temperature Trends

Deforestation, agriculture and dam development trends were analyzed and compared directly to number of warm LWST days and warm LWST nights per year utilizing the MODIS LWST and IGBP/MODIS land cover datasets for the available period between 2003 and 2017. During this period, total agriculture land in the lake's floodplain increased by approximately 245 km2, and forest cover decreased by approximately 1220 km^2. Much of the deforested area was converted into woody savannah, grassland and permanent wetland according to classifications developed by IGBP. However, as noted in the product's user-guide, cropland in the immediate lake's floodplain are likely underestimated. The NW TSL region was also found to frequently be cooler than the SE TSL region for most dry-season days during this period from the MODIS LWST data. An example of this can be observed in Figure 4.7, which shows a map of the annual average temperature across the lake and its floodplain for 2003, 2015 and the difference between the two years.

The number of warm LWST days per year (days above long-term average) as observed by MODIS satellites, normalized by sample size is plotted against the area of agriculture and forest in the lake's floodplain in Figure 4.8. Both plots demonstrate correlations between the number of warm days per year and the land cover type in the lake's floodplain. The highest correlation is between increased agriculture area and increased amounts warm days, particularly in the SE region ($R^2 = 0.61$), indicating the lake's warming trends are likely linked to these land cover changes. In both plots, the SE region of the lake shows a stronger correlation between the amount of agriculture and forested area than the NW region. Insignificant correlation was found between land cover and warm nights per year, thus, they are not shown in Figure 4.8.

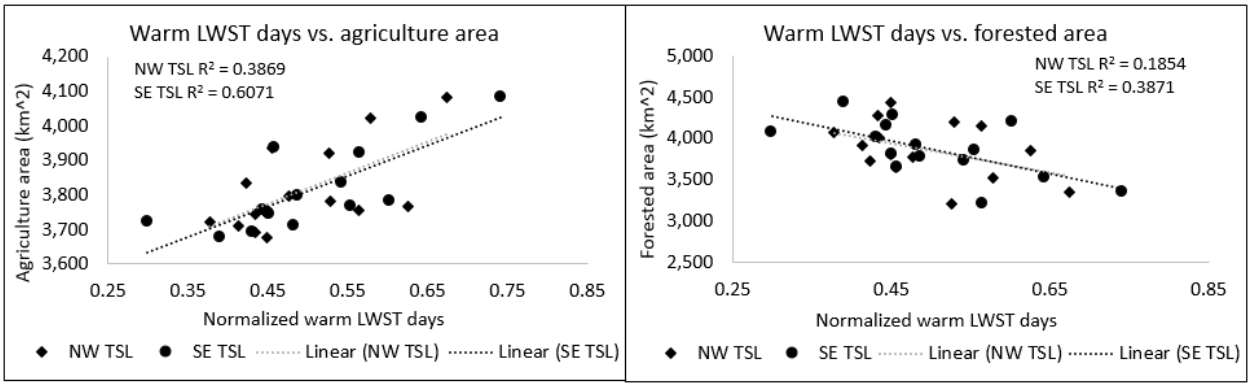

Figure 4.8. Plots of the number of warm surface water temperature days and nights normalized by sample size per year and a) agriculture area and b) forest area in the lake's floodplain. Temperature data from MODIS Aqua satellite and land cover data from IGBP for the available time period of 2003 – 2017.

Dam development in the entire Mekong River basin increased volumetric storage behind dams by 72 km^3 between 2003 and 2008. The largest dams were built in China on the Mekong mainstem in 2010 and 2014, damming approximately 24 km^3 and 15 km^3, respectively. Cumulative storage behind dams constructed in the Mekong River Basin was compared annually to number of warm days per year in both the Tonle Sap Lake and the Mekong River near the Tonle

Sap River confluence. Figure 4.9 shows cumulative volume stored behind dams constructed since 2003, and warm anomalies in both the Tonle Sap Lake and Mekong River analysis regions. While Mekong River shows a decreasing trend in the number of warm days experienced during the dry-season of each year, Tonle Sap's LWST trends show an increase in number of warm days per year at a rate higher than air temperature. The normalized warm days per year are fairly similar between the two systems from 2003 through 2014. The deviation begins in 2015 coinciding with a major dam development in 2014. Interestingly, both Tonle Sap Lake and the Mekong River show an approximate equal rate in increase of number of warm nights per year that mirrors the trend in air temperature.

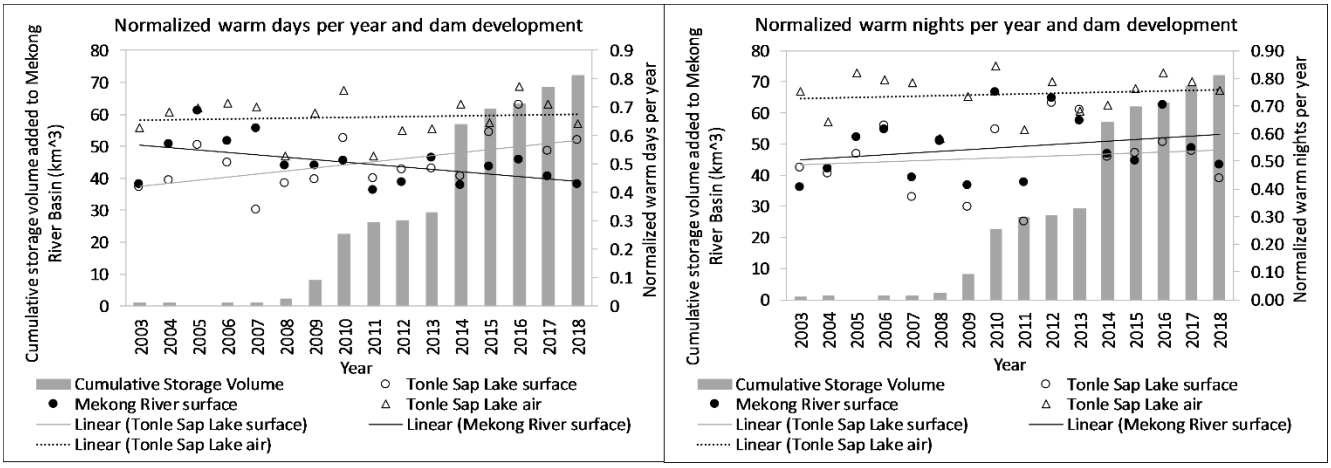

Figure 4.9. Plot showing the annual cumulative storage added to the Mekong River Basin since 2003, and number of warm surface water temperature days per year (normalized by sample size) for Tonle Sap Lake air (Reanalysis data) and surface temperature and Mekong River surface temperature (MODIS Aqua data).

Larger year to year decreases in the number of warm days in the Mekong River occurred within a year or two of relatively large increases in cumulative storage held behind the dams. However, this should be interpreted with caution as many variables influence a river's thermal trends including how the dams were actually operated. Also, it should be noted that the largest

year-to-year decrease in number of warm days in the Mekong River occurred between 2007 and 2008, when little storage volume was added to the system. This may be influenced by operations of dams existing prior to 2003 or a relatively cool climate throughout the region, both are not analyzed as part of this study.

The next chapter discusses the conclusion and recommended next steps for understanding and managing Tonle Sap Lake's thermal regime and watershed impacts to its natural thermal regime. Conclusions drawn in Chapter 4 are determined from the background work described in Chapter 2 and results described in Chapter 3. Recommendations for future work are largely drawn from areas of the methodology where improvement can be made, described in Chapter 3.

Chapter 5. DISCUSSION, CONCLUSION AND RECOMMENDATIONS

5.1 DISCUSSION AND CONCLUSION

The Tonle Sap Lake's hydrological and ecological resources are the lifeblood of the Mekong region and it is currently warming in sync with the regional climate. Schneider and Hook (2010) found over one hundred lakes around the world to be warming at a rate of 0.045°C yr^{-1} on average, and Tonle 256 Sap Lake follows close suite with an average dry-season warming rate of 0.03°C yr^{-1}. Tonle Sap's LWST temperature trends also follow local air temperature trends, as expected for a large, shallow lake. Tonle Sap Lake and its floodplain have been experiencing heavy exploitation of resources for at least several decades (Campbell, Poole, Giesen, & Valbo-Jorgensen, 2006) and the newly observed warming trends here adds additional concerns over the future ability of ecosystem to provide services to society. A recent study examining tropical fish (include species from the Tonle Sap) physiological response to warming under controlled conditions indicated an unexpected tolerance and ability to perform at water temperatures up to 4 ˚C above current maxima (Lapointe, et al., 2018). While encouraging from the perspective of individual fish, temperature is a critical ecological variable that impacts ecosystems at all levels of organization, from genes to biogeochemical cycles, and there is evidence that temperatures above optimal for fish health can lead to habitat loss, a shift towards smaller body sizes and ultimately loss in ecosystem function (Walberg, 2011).

Beyond the direct observation of recent warming, this study also found significant correlations between deforestation and increased agriculture development and the lake's warming trends. This suggests that the thermal regime of the lake is highly sensitive to local land use and agricultural practices. Land use change from forest to agriculture is expected to continue in the

region as the lower basin countries pursue policies of increased rice export. While troubling in the near term, coupling of land use and lake temperature also presents opportunity for coordinated forest restoration and agricultural management as a potential mitigation strategy to lessen the lake's warming trends, a strategy that has shown success in many parts of the world (Cunningham, et al., 2015).

The continued and seemingly inevitable development of hydropower dams remains a major concern for Tonle Sap ecosystem. Thus, it is imperative that they are designed to minimize impacts to downstream systems, including Tonle Sap Lake. It remains to be assessed if dams can be designed to send cooler waters downstream as a potential management strategy that could potentially help to mitigate the warming trends observed in Tonle Sap Lake. Correlation between the Tonle Sap Lake temperature trends and dam development is currently low. However, it is difficult to conclude if further development will show a clear impact especially as more dams are constructed on the main stem of the Mekong river and closer to the lake. For now, it is yet to be determined if existing hydropower schemes are warming or cooling 283 downstream river waters. Further exploration into this would help local water resource managers to identify vulnerabilities of schemes and land use practices that intensify warming trends, or opportunities to manage these schemes to maintain a stable thermal regime in Tonle Sap Lake.

Temperature is a fundamental parameter in natural and managed ecosystems that are the basis of rural livelihoods globally. Natural thermal regimes around the world are being disrupted by patterns of global warming, and results from this study newly identifies the Tonle Sap Lake's thermal regime is warming as well. This study shows that warming air temperatures are likely driving some of the thermal regime changes in Tonle Sap Lake. Many lakes around the world, appear to be warming faster than their regional air temperatures, however, Tonle Sap Lake appears

to be warming at the same rate as the regional air temperatures. Climate change impacts may only exacerbate the impairment of the lake's hydrologic and biotic systems. It is imperative that the impacts of this to biological species in the lake's ecosystem are understood, as their populations are already declining.

5.2 Recommendations for Future Work

This study revealed that temperature trends in Tonle Sap Lake are warming, and that the Mekong River temperature trends were following suite historically but may be diverging in recent years. Further exploration into temperature trends along the Mekong River, particularly in areas nearby hydropower schemes should be investigated. In addition to investigating temperature trends, understanding how these hydropower schemes are influencing the seasonal hydrograph should be understood, as that can greatly impact ecosystems.

Investigation into some of the variables analyzed in this study could be improved upon. The one that may be of most benefit for water resource management would be improving land cover classification and documentation and mapping of land use in the floodplain, particularly areas of agriculture operations. The IGBP dataset employed in this analysis provides a high-level estimate of land cover in the region, but some inaccuracies were highlighted, and further efforts are still needed to accurately portray land use development in Tonle Sap Lake's floodplain. Developing an improved, supervised classification algorithm utilizing Landsat or MODIS sensor data in the visible spectrum could be conducted. Also, leveraging upon the IGBP data by ground-truthing the data through in-situ mapping efforts could also help to improve understanding of agricultural operations that are changing the landscape in Tonle Sap Lake's floodplain.

Lastly, LWST and air temperature data could be improved upon with better in-situ data to calibrate each satellite remote sensing dataset. Improving these two datasets could help identify

other trends occurring in Tonle Sap Lake. Another area that the lake's temperature is likely impacting include microclimate effects, which understanding could be improved upon with better quality air temperature. Further studies are also recommended to understand the processes that may be driving deforestation and agriculture to coincide with warming of the lake to help identify potential mitigation strategies. Improving in-situ monitoring of the lake's temperatures, particularly around agricultural operations and forested areas would greatly help improve understanding of how these different land covers are directly impacting the lake's thermal regime.

REFERENCES

Adrian et al., R. (2009). Lakes as sentinels of climate change. *Limnol. Oceanogr., 54*.

Arias, M., Cochrane, T., Piman, T., Kummu, M., Caruso, B., & Killeen, T. (2012). Quantifying changes in flooding and habitats in the Tonle Sap Lake (Cambodia) caused by water infrastructure development and climate change in the Mekong Basin. *Journal of Environmental Management 112,* 53-66.

Baker-Yeboah, S., Saha, K., Zhang, D., Casey, K., Evans, R., & Kilpatrick, K. (2016). Pathfinder Version 5.3 AVHRR Sea Surface Temperature Climate Data Record. *Fall AGU Poster*.

Baran, E., & Myschowoda, C. (2009). Dams and fisheries in the Mekong Basin. *Aqua. Ecosystem Health Management. 12*, 227-234.

Bengtsson, L. (2012). *Thermal Regime of Lakes.* Springer Netherlands: Encycloperia of Earth Sciences Series.

Beschta, R. (1997). Riparian shade and stream temperature: an alternative perspective. *Rangelands 19*, 25-28.

Bonnema, M., & Hossain, F. (2017). Inferring reservoir operating patterns across the Mekong Basin using only space observations. *Water Resources Research 53*.

Brown. (2004). *Outgrowing the earth: the food security problem in an age of failing water tables and rising temperatures.* New York: Earth Policy Institute.

Brown, G. W., & Krygier, J. T. (1970). Effects of clear-cutting on stream temperature. *Water Resources Research 6*, 1133-1139.

Caissie, D. (2006). The thermal regime of rivers: a review. *Freshwater Biology*, 51: 1389-1406.

Campbell, I., Poole, C., Giesen, W., & Valbo-Jorgensen, J. (2006). Species diversity and ecology of Tonle Sap Great Lake, Cambodia. *Aquatic Sciences 68*, 355 - 373.

Clarke, A., & Gaston, K. (2006). Climate, energy and diversity. *Proc R Soc Lond B Biol Sci.*, 273: 2257 - 2266.

Cochrane, T., Arias, M., & Piman, T. (2014). Historical impact of water infrastructure on water levels of the Mekong River and the Tonle Sap System. *Hydrology and Earth System Sciences 18*, 4529-4541.

Commission, M. R. (2003). *State of the Basin Report.* Phnom Penh: Mekong River Commission.

Commission, M. R. (2011). Hydrological Database. Vientiane Lao PDR.

Commission, M. R. (2011). *Hydrological/Water Quality Database.* Phnom Penh: Mekong River Commission.

Cunningham, S.C., M. N., R., B., P.J., C., T.R., B., J., T. J., & Thompson, R. (2015). Balancing the environmental benefits of reforestation in agricultural regions. *Perspective in Plant Ecology, Evolution and Systematics 17*, 301-317.

Evans, E., McGregor, G., & Petts, G. (1998). River energy budgets with special reference to river bed processes. *Hydrol Process*, 12: 575-595.

Ficke, A., Myrick, C., & Hansen, L. (2007). Potential impacts of global climate change on freshwater fisheries. *Rev Fish Biol Fisher 17*, 581-613.

Friedl, M., & Sulla-Menashe, D. (2015). MCD12Q1 MODIS/Terra+Aqua Land Cover Type Yearly L3 Global 500m SIN Grid V006. *NASA EOSDIS Land Processes DAAC*.

Ghent, D. (2012). Land surface temperature validation and algorithm verification. *Report to European Space Agency*, 1-17.

Haddeland, I., Lettenmaier, D. P., & Skaugen, T. (2006). Effects of irrigation on the water and energy balances of the Colorado and Mekong river basins. *Journal of Hydrology 324*, 210-223.

Holtgrieve, G. (n.d.). Tonle Sap Lake Temperature Observation data. unpublished data.

Holtgrieve, G., Arias, M., Irvine, K., Lamberts, D., Ward, E., Kummu, M., . . . Richey, J. (2013). Patterns of Ecosystem Metabolism in the Tonle Sap Lake, Cambodia with Links to Capture Fisheries. *PLoS ONE 8(8)*.

Hortle, K. G. (2007). *Consumption and the yield of fish and other aquatic animals from the Lower Mekong Basin.* Vientiane, Lao: Mekong River Commission.

Hulley, G., Hook, S., & Schneider, P. (2011). Optimized split-window coefficients for deriving surface temperatures from inland water bodies. *Remote Sensing of Environment*(115), 3758-3769.

Ilha, P., Schiesari, L., Yanagawa, F., Jankowski, K., & Navas, C. (2018). Deforestation and stream warming affect body size of Amazonian fishes. *PLoS ONE 13*.

Ishikawa, S., Hori, M., & Kurokura, H. (2017). A Strategy for Fisheries Resources Management in Southeast Asia: A Case Study of an Inland Fishery around Tonle Sap Lake in Cambodia. *Aqua-Bioscience Monographs, 10*(2), 23-40.

Janzen, D. (1967). Why mountain passes are higher in the tropics. *American Naturalist 101*, 233-246.

Jin, M., & Treadon, R. (2003). Correcting the orbit drift effect on AVHRR land surface skin temperature measurements. *Internation Journal of Remote Sensing*, 4543-4558.

Johnson, S. L., & Jones, J. A. (2000). Stream temperature response to forest harvest and debris flows in western Cascades, Oregon. *Canadian Journal of Fisheries and Aquatic Sciences 57 (Suppl. 2)*, 30-39.

Kalnay et al. (1996). The NCEP/NCAR 40-Year Reanalysis Project. *Bull. Amer. Meteor. Soc. 77*, 437-471.

Kummu, M., & Sarkkula, J. (2008). Impacts of the Mekong River Flow Alteration on the Tonle Sap Flood Pulse. *Ambia 37*, 185-192.

Kummu, M., Jozsa, J., Sarkkula, J., & Koponen, J. (2014). Water balance analysis for the Tonle Sap Lake-Floodplain system. *Hydrological Processes*.

Kummu, M., Penny, D., Sarkkula, J., & Koponen, J. (2008). Sediment: Curse or Blessing for Tonle Sap Lake? *Springer on behalf of Royal Swedish Academy of Sciences*, 158-163.

Lapointe, D., Cooperman, M. S., Chapman, L. J., Clark, T. D., Val, A. L., Ferreira, M. S., . . . Cooke, S. J. (2018). Predicted Impacts of climate warming on aerobic performance and upper thermal tolerance of siz tropical freshwater fishes spanning three continents. *Conserv Physiol 6(1)*.

Lapointe, D., M.S., C., L.J., C., T.D., C., A.L., V., M.S., F., . . . S.J., C. (2018). Predicted impacts of climate warming on aerobic performance and upper thermal tolerance of six tropical freshwater fishes spanning three continents. *Conserv Physiol*.

Lawrence, D., & Vandecar, K. (2014). Effects of tropical deforestation on climate and agriculture. *Nature Climate Change (5)*.

Lehner, B., Verdin, K., & Jarvis, A. (2008). New global hydrography derived from spaceborne elevation data. *Eos, Transactions, AGU*, 93-94.

Macedo, M., Coe, M., Defries, R., Uriarte, M., Brando, P., Neill, C., & et al. (2013). Land-use-driven stream warming in southeastern Amazonia. *Philos Trans R Soc Lond B Biol Sci.*, 368.

Manton et al., M. (2001). Trends in Extreme Daily Rainfall and Temperature in Southeast Asia and the South Pacific: 1961 – 1998. *International Journal of Climatology 21*, 269-284.

Maul, G., & Sidran, M. (1971). Estimation of sea surface temperature from space. *Remote Sensing of Environment*(2), 165-169.

McCully, P. (2001). *Silenced rivers: The ecology and politics of large dams.* London: Zed Books.

Metz, M. R. (2014). Surface Temperatures at the Continental Scale: Tracking Changes with Remote Sensing at Unprecedented Detail. *Remote Sensing 6*, 3822-3840.

Miller, B. (2015). Unpublished data.

Niemeyer, R., Cheng, Y., Mao, Y., Yearsley, J., & Nijssen, B. (2018). A Thermally Stratified Reservoir Module for Large-Scale Distributed Stream Temperature Models With Application in the Tennessee River Basin. *Water Resources Research*, 8103-8119.

Osborne, M. (2006). *Mekong: Turbulent Past, Uncertain Future.* Allen & Unwin.

Oyagi, H., Endoh, S., Ishikawa, T., Okumura, Y., & Tsukawaki, S. (2017). Seasonal Changes in Water Quality as Affected by Water Level Fluctuations in Lake Tonle Sap, Cambodia. *Geographical Review of Japan*, 53-65.

Pareeth, S., Salmaso, N., Adrian, R., & Neteler, M. (2016). Homogenised daily lake surface water temperature data generated from multiple satellite sensors: A long-term case study of a large sub-Alpine lake. *Scientific Reports 6*.

Price, J. (1991). Timing of NOAA afternoon passes. *Internation Journal of Remote Sensing 12*, 193-198.

Rosenberg, D., McCully, P., & Pringle, C. (2000). Global-scale environmental effects of hydrological alterations: Introduction. *Bioscience 50(9)*, 746-751.

Ruiz-Barradas, A., & Nigam, S. (2018). Hydroclimate Variability and Change over the Mekong River Basin: Modeling and Predictability and Policy Implications. *American Meteorolgoical Society*, *19*, 849 - 869.

Schneider, P., & Hook, S. (2010). Space observations of inland water bodies show rapid surface warming since 1985. *Geophysical Research Letters 37*.

Sen, P. (1968). Estimates of the Regression Coefficient Based on Kendall's Tau. *Journal of the American Statistical Association 63*, 1379-1389.

Silverio, D., Brando, P., Macendo, M., Beck, P., Bustamante, M., & Coe, M. (2015). Agricultural expansion dominates climate changes in southeastern Amazonia: the overlooked non-GHG forcing. *Environ Red Lett*, 10: 104015.

Simon, R., Tormos, T., & Danis, P. (2014). Retrieving water surface temperature from archive LANDSAT thermal infrared data: Application of the mono-channel atmospheric correction algorithm over two freshwater reservoirs. *Int. J. Appl. Earth Obs. Geoinf*(30), 247-250.

Stillman, J. (2003). Acclimation capacity underlies susceptibility to climate change. *Science 301*, 65.

Survey, U. G. (2016). Landsat – Earth observation satellites. *U.S. Geological Survey Fact Sheet*, 2015-3081.

U.S. Geological Survey. (2016). Landsat - Earth observation satellites. *U.S. Geological Survey Fact Sheet*, 2015-3081.

van Zaline, N. (2002). Update on the status of the Cambodian inland capture fisheries sector with special reference to the Tonle Sap Great Lake. *Mekong Fish Catch and Culture 8*.

Walberg, E. (2011). Effect of Increased Water Temperature on Warm Water Fish Feeding Behavior and Habitat Use. *Journal of Undergraduate Research at Minnesota State University, Mankato 11*.

Wan, Z., Hook, S., & Hulley, G. (2015). MYD11A1 MODIS/Aqua Land Surface Temperature/Emissivity Daily L3 Global 1km SIN Grid V006 LST. . *NASA EOSDIS LP DAAC*.

Wassmann, R., Hien, N., & Hoanh, C. (2004). *Climate Change, 66*(1-2), 89-107.

WLE. (2017). *Dataset on the Dams of the Irrawaddy, Mekong, Red and Salween River Basins.* Vientiane: CGIAR Research Program on Water, Land and Ecosystems - Greater Mekong.

Wright, S., Holly, F., Bradley, A., & Krajewski, W. (1999). Long-term simulation of thermal regime of Missouri River. *ASCE Journal of Hydraulic Engineering*(125), 242-252.

Yen, N., Sunada, K., Oishi, S., Sakamoto, Y., Ikejima, K., & Iwata, T. (2008). The Spatial Distribution of Fish Species Catches in Relation to Catchment and Habitat Features in the Floodplain Lot Fisheries of Tonle Sap Lake, Cambodia. *Journal of Fisheries and Aquatic Science 3*, 2013-227.

APPENDIX A. SUPPLEMENTAL DATA

Table A.1 Data for Dam Development in the Mekong River Basin

Year	Cumulative Number of Dams	Cumulative Storage Capacity Added (m^3)
1956	2	513
1959	3	1583
1965	4	1749
1966	5	4308
1967	6	4418
1968	7	5758
1970	9	5758
1971	12	12439
1972	13	12604
1973	14	13124
1974	15	13434
1976	16	13434
1977	17	13544
1979	18	13544
1980	19	13685
1981	20	13727
1982	22	13899
1984	23	14012
1987	24	14012
1988	27	14385
1989	28	14442
1990	29	14442
1992	31	15388
1994	34	15388
1995	36	15450
1996	38	15450
1997	39	16542
1998	41	16561
1999	43	20165
2000	44	20350
2001	45	21423
2003	46	22313
2004	49	22513
2006	50	22513
2007	55	22513
2008	58	23586
2009	67	29349
2010	72	44001
2011	76	47630
2012	81	48263
2013	82	50713

2014	87	78169
2015	94	83196
2016	104	84753
2017	116	90016
2018	124	93440
2019	136	97826
2020	160	111161
2021	165	111259
2022	170	111259
2023	172	112298
2024	173	112298
2026	177	113777
2030	180	115366

[Source: WLE, 2017]

Table A.2 In-situ temperature data for Prek Konteil site 1

In-Situ Prek Konteil 1

GPS	Date	Time	Transducer Depth (m)	Water T (°C)
N 13.07350 E 103.71883	5-Nov-2015	7:46	0.214	30.29
			0.409	30.30
			0.622	30.30
			0.870	30.29
			1.148	30.29
			1.376	30.29
			1.601	30.29
			1.914	30.29
			2.122	30.30
			2.354	30.31
			2.604	30.31
			2.847	30.31
			3.076	30.31
			3.276	30.30
			3.427	30.26
			3.530	30.26

Table A.3 In-situ temperature data for Prek Konteil site 2

In-Situ Prek Konteil 2

GPS	Date	Time	Transducer Depth (m)	Water Temperature (°C)
N 13.06167 E 103.69593	5-Nov-2015	10:34	0.251	30.62
			0.397	30.53
			0.666	30.40
			0.876	30.36
			1.108	30.33
			1.366	30.31
			1.622	30.31
			1.877	30.30
			2.080	30.30
			2.368	30.29
			2.648	30.29
			2.912	30.29
			3.153	30.29
			3.353	30.29
			3.497	30.29
			3.574	30.29
			3.672	30.29

Table A.4 In-situ temperature data for Prek Konteil site 3

In-Situ Prek Konteil 3

GPS	Date	Time	Transducer Depth (m)	Water T (°C)
N 13.06082 E 103.68385	6-Nov-2015		0.222	29.37
			0.317	29.49
			0.562	29.17
			0.844	29.11
			1.073	29.09
			1.267	29.08
			1.588	29.06
			1.779	29.05
			2.116	29.03
			2.322	29.02
			2.599	29.01
			2.812	29.01

Table A.5 In-situ temperature data for Prek Konteil site 4

In-Situ Prek Konteil 4

GPS	Date	Time	Transducer Depth (m)	Water T (°C)
N 13.05496 E 103.68333	6-Nov-2015		0.201	28.60
			0.343	29.52
			0.613	29.40
			0.860	29.37
			1.109	29.35
			1.327	29.34
			1.566	29.33
			1.847	29.32

Table A.6 In-situ temperature data for Prek Konteil site 5

In-Situ Prek Konteil 5

GPS	Date	Time	Transducer Depth (m)	Water T (°C)
N 13.04305 E 103.66675	5-Nov-2015	14:40	0.214	29.51
			0.376	29.64
			0.620	29.41
			0.696	29.30

Table A.7 In-situ temperature data for Anlang Reang site 1

In-Situ Anlang Reang 1

GPS	Date	Time	Transducer Depth (m)	Water T (°C)
N 12.65388 E 104.16687	4-Oct-2015		0.244	29.88
			0.510	29.88
			0.775	29.88
			1.041	29.88
			1.306	29.88
			1.572	29.88
			1.837	29.88
			2.103	29.88
			2.368	29.88
			2.634	29.88
			3.326	29.88
			3.583	29.88
			3.840	29.88
			4.080	29.88
			4.320	29.88
			4.566	29.88
			4.811	29.87
			5.080	29.88
			5.320	29.88

Table A.8 In-situ temperature data for Anlang Reang site 2

In-Situ Anlang Reang 2

GPS	Date	Time	Transducer Depth (m)	Water T (°C)
	4-Oct-			
N 12.65222	2015		0.194	30.31
E 104.14899			0.366	30.14
			0.578	30.05
			0.847	29.98
			1.044	29.96
			1.390	29.95
			1.831	29.88
			2.099	29.83
			2.314	29.75
			2.545	29.67
			2.843	29.52
			3.085	29.39
			3.316	29.10
			3.521	28.97
			3.812	28.87

Table A.9 In-situ temperature data for Anlang Reang site 3

In-Situ Anlang Reang 3

GPS	Date	Time	Transducer Depth (m)	Water T (°C)
	4-Oct-			
N 12.64576	2015		0.242	28.94
E 104.14134			0.424	28.85
			0.649	28.81
			0.893	28.79
			1.158	28.79
			1.396	28.79
			1.600	28.79

Table A.10 In-situ temperature data for Anlang Reang site 4

In-Situ Anlang Reang 4

GPS	Date	Time	Transducer Depth (m)	Water T (°C)
N 12.64003 E 104.13542	4-Oct-2015		0.219	28.38
			0.440	28.26
			0.655	28.21
			0.898	28.15
			1.154	28.12
			1.412	28.04
			1.651	27.95
			1.901	27.91
			2.138	27.90
			2.392	27.89
			2.654	27.85
			2.874	27.86
			3.141	27.85

Table A.11 In-situ temperature data for Anlang Reang site 5

In-Situ Anlang Reang 5

GPS	Date	Time	Transducer Depth (m)	Water T (°C)
N 12.63007 E 104.12852	4-Oct-2015		0.174	29.14
			0.355	28.56
			0.624	28.18
			0.885	28.05
			1.100	27.94
			1.267	27.90

Table A.12 In-situ temperature data for Anlang Reang site 6

In-Situ Anlang Reang 6

GPS	Date	Time	Transducer Depth (m)	Water T (°C)
	4-Oct-			
N 12.62540	2015		0.209	29.68
E 104.12143			0.335	29.58
			0.560	29.42
0.31			0.662	29.37

Table A.13 In-situ temperature data for Chnouk Tru site 1

In-Situ Chnouk Tru 1

GPS	Date	Time	Transducer Depth (m)	Water T (°C)
	27-Oct-			
N 12.5128286	2015	12:00	0.192	31.79
E 104.48664			0.320	31.52
			0.649	31.11
			0.884	30.99
			1.127	30.80
			1.376	30.64
			1.674	30.63
			1.882	30.61
			2.115	30.57
			2.599	30.58
			3.133	30.57
			3.595	30.56
			4.103	30.56
			4.531	30.55
			5.059	30.55
			5.570	30.55
			5.741	30.55
			5.826	30.54

Table A.14 In-situ temperature data for Chnouk Tru site 2

In-Situ Chnouk Tru 2

GPS	Date	Time	Transducer Depth (m)	Water T (°C)
N 12.51012	27-Oct-2015	9:30	0.280	30.64
E 104.48435			0.450	30.65
			0.730	30.66
			0.958	30.67
			1.203	30.67
			1.441	30.67
			1.991	30.67
			2.142	30.67
			2.417	30.68
			2.677	30.68
			2.906	30.65
			3.137	30.67

Table A.15 In-situ temperature data for Chnouk Tru site 3

In-Situ Chnouk Tru 3

GPS	Date	Time	Transducer Depth (m)	Water T (°C)
N 12.50553	28-Oct-2015		0.213	30.84
E 104.47363			0.426	30.67
			0.630	30.41
			0.895	30.33
			1.141	30.29
			1.385	30.28
			1.634	30.26
			1.864	30.25
			2.123	30.24
			2.380	30.23
			2.466	30.21

Table A.16 In-situ temperature data for Chnouk Tru site 4

In-Situ Chnouk Tru 4

GPS	Date	Time	Transducer Depth (m)	Water T (°C)
N 12.49585 E 104.47293	28-Oct-2015	12:02	0.215	31.52
			0.376	31.02
			0.641	30.83
			0.909	30.72
			1.137	30.67
			1.395	30.59
			1.608	30.57
			1.876	30.53
			2.066	30.51
			2.353	30.48
			2.480	30.46
			2.568	30.42
			2.624	30.42

Table A.17 In-situ temperature data for Chnouk Tru site 5

In-Situ Chnouk Tru 5

GPS	Date	Time	Transducer Depth (m)	Water T (°C)
N 12.48966 E 104.46839	27-Oct-2015		0.175	31.59
			0.390	31.03
			0.667	30.62
			0.883	30.51
			1.082	30.41
			1.393	30.33
			1.600	30.25
			1.843	30.21
			1.974	30.18

Table A.18 In-situ temperature data for Chnouk Tru site 6

In-Situ Chnouk Tru 6

GPS	Date	Time	Transducer Depth (m)	Water T (°C)
N 12.48377 E 104.46389	28-Oct-2015	10:53	0.265 0.304	29.19 29.16